Multi-scale modeling of low-density carbon-phenolic ablators

Nagi N. Mansour

Chief division scientist

NASA Advanced Supercomputing (NAS) division

Contributors

Jeremie Meurisse

Francesco Panerai ⟹ UIUC

Jean Lachaud ⟹ U. Bordeuax

Joseph Ferguson ⟹ PhD program Stanford U.

Arnaud Boner

Federico Semeraro

Brody Bessire

John Thornton

Joshua Monk

Mona Karimi

Patricia Ventura

Seokkwan Yoon

Sander Visser

Francisco Torres-Herrador

JB Scoggins ⟹ VKI/Ecole Polytechnique

Thierry Magin ⟹ VKI

Marco Panesi

Kelly Stefani

Alexandre Martin

Tim Sandstron

Alastair MacDowell

Dula Parkinson

Harold Barnard

Tim Minton

Others that I have missed to whom I apologize

+ **Many NASA summer interns**

Entry stage of planetary Exploration

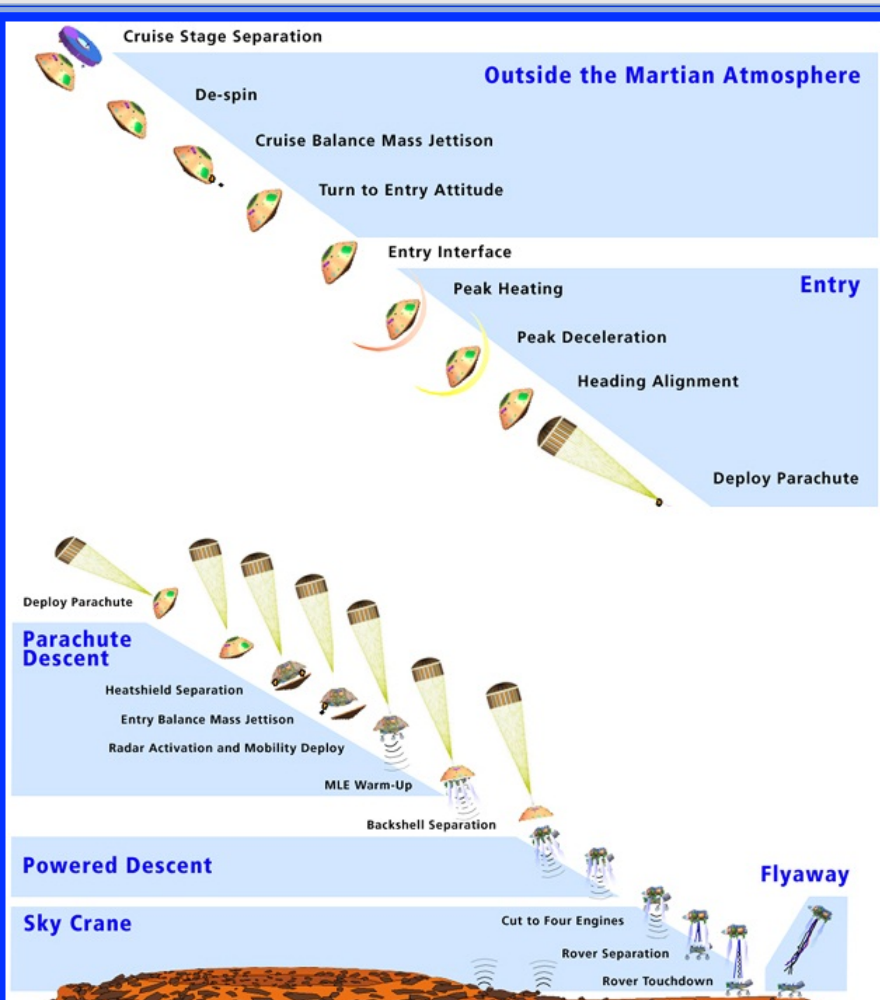

Entry stage of planetary Exploration is a core competency element at NASA Ames Research Center (ARC)

NASA atmospheric entry missions supported at ARC

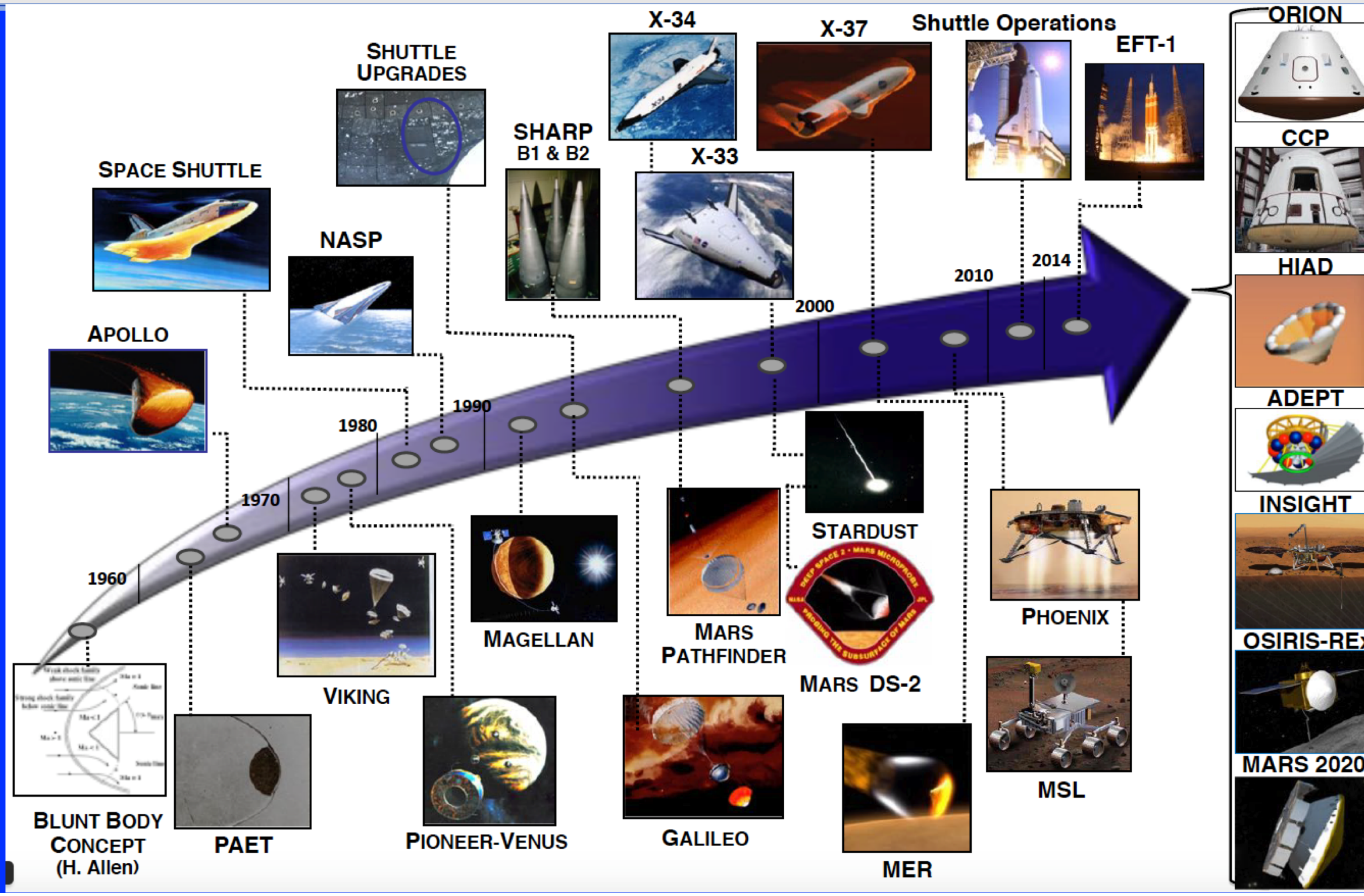

Choosing the TPS Material

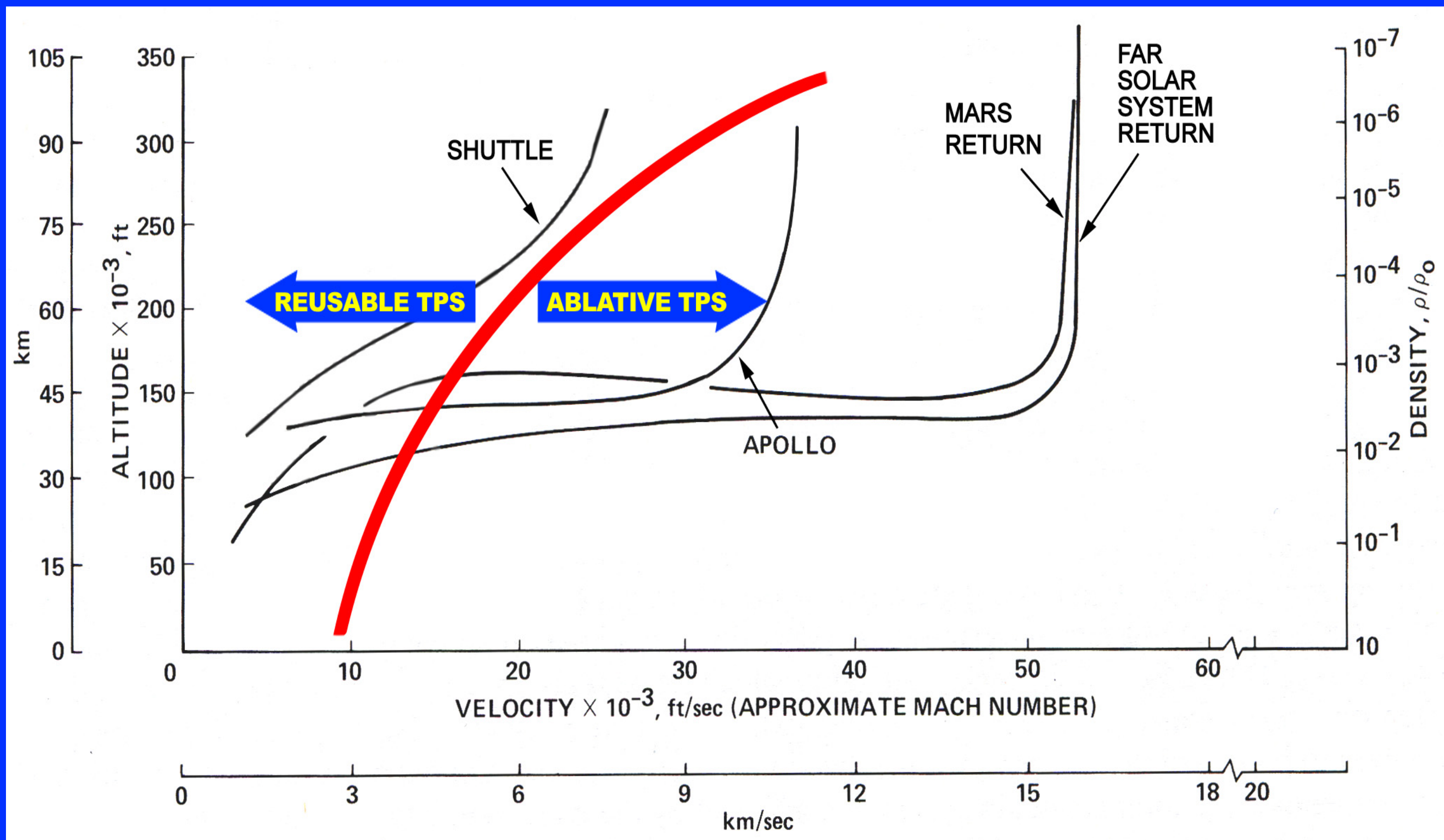

Missions requiring ablative heatshield may employ reusable TPS on regions of vehicle with low heating

Arc Jet tests: Meteorite Ablation

Courtesy: E. Stern et al. 2018

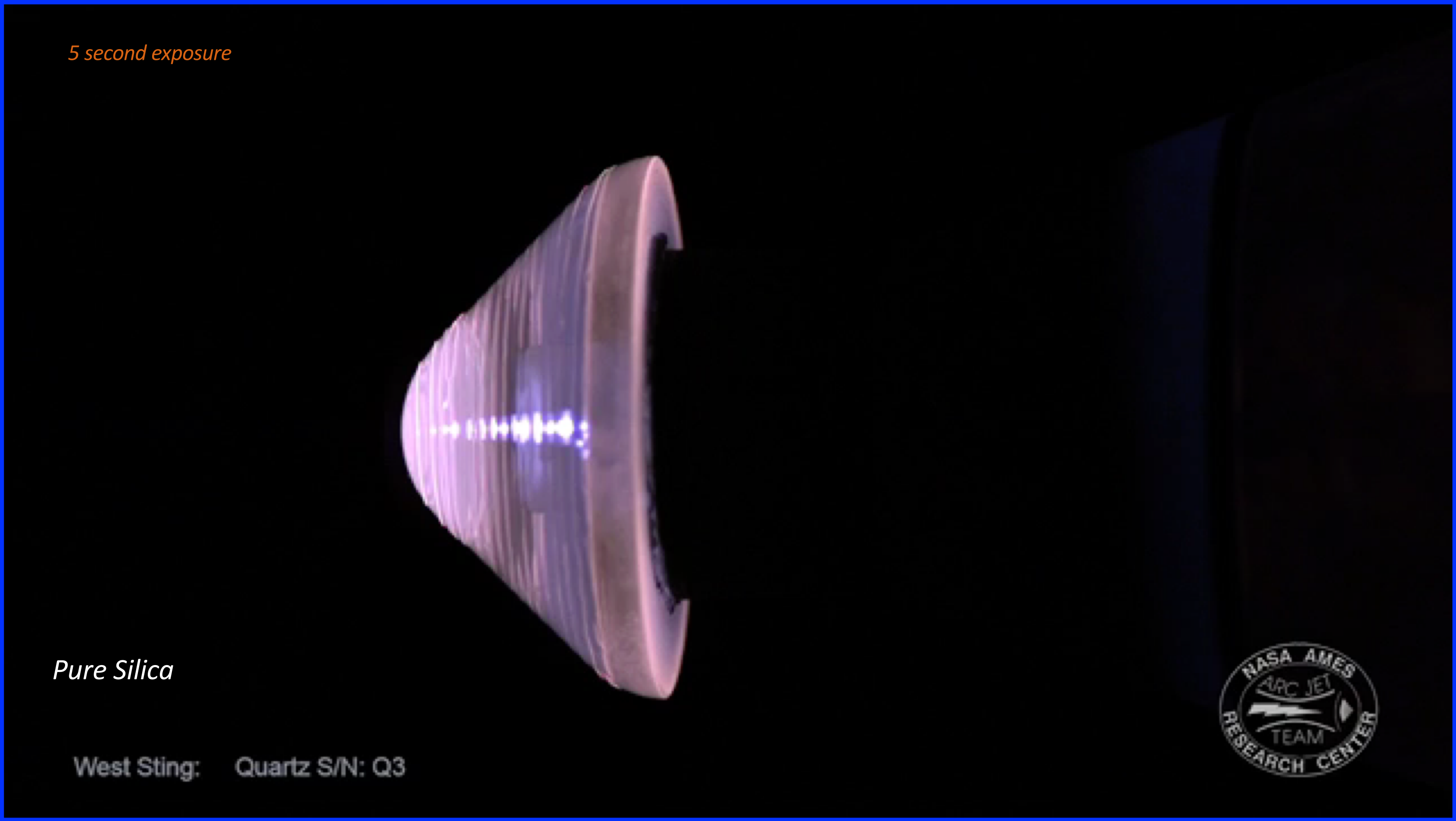

Focus: Porous Carbon Ablators

Phenolic Impregnated Carbon Ablator (PICA) Class Focus

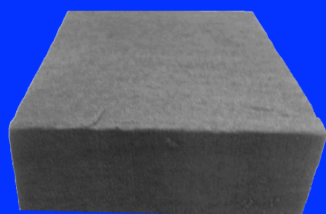

Carbon Preform

+

Resin
Infiltration (Phenolic)

=

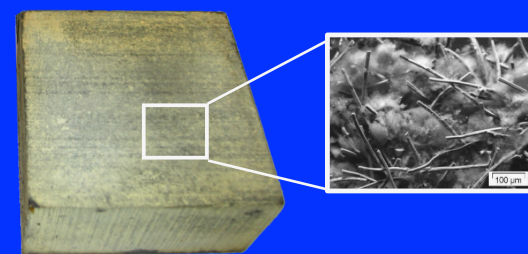

Ablator

Major “Species” :

PICA

CPICA

HEEET

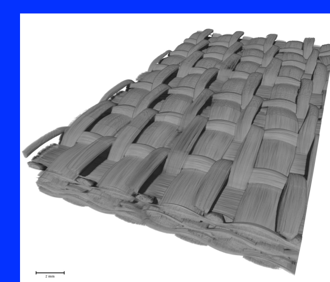

Carbon Weave

Broadly applicable, relatively simple chemistry. Start here and work towards more complex systems

Mission Applications

Stardust (1999)

MSL (2012)
Mars 2020

SpaceX Dragon
(operational)

OSIRIS-Rex
(2016)

⇒ HEEET incentivized in current Discovery and New Frontiers Proposal Calls

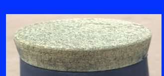

⇒ Working on providing Conformal PICA as incentivized technology as well

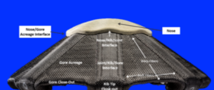

⇒ ADEPT is a candidate technology for Venus and Human Mars

Highly reliable Mars Sample Return development requires high fidelity modeling

Macro-scale range of scales (environment)

Smooth OML flight environments

Laminar　　　　Turbulent

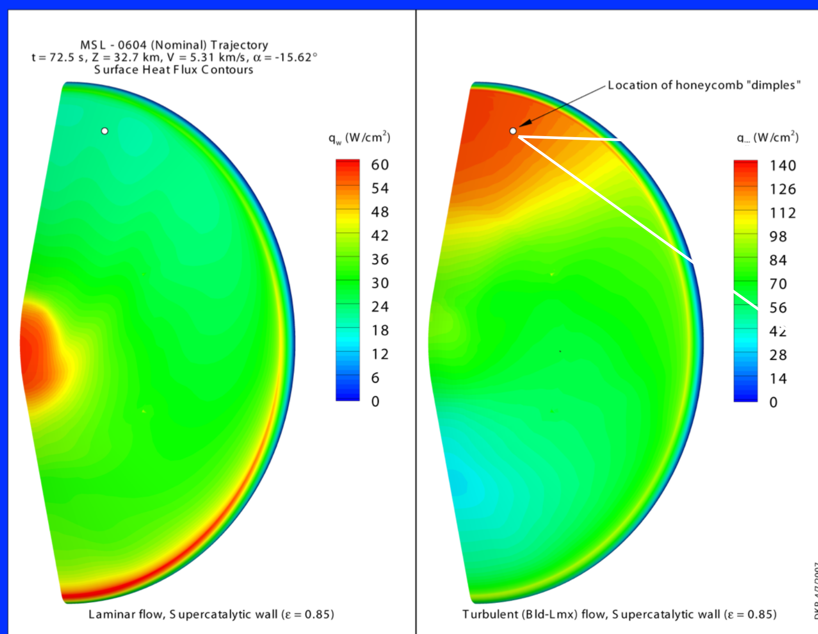

O(m)

Heating augmentation from exposed honeycomb
(two orientations - ≈1mm max. depth)

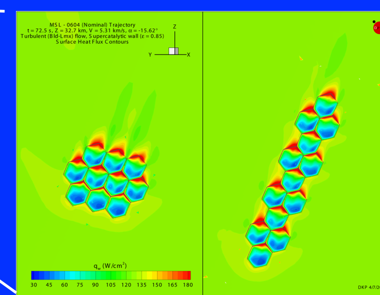

O(cm)

Courtesey D. Prabhu, 2007

Range of scales (materials)

O(cm)

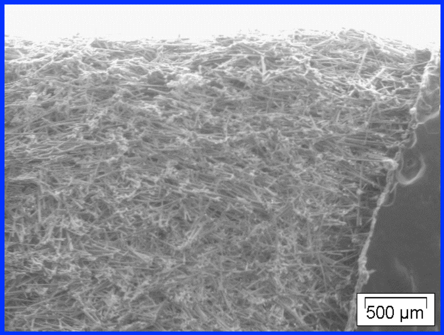

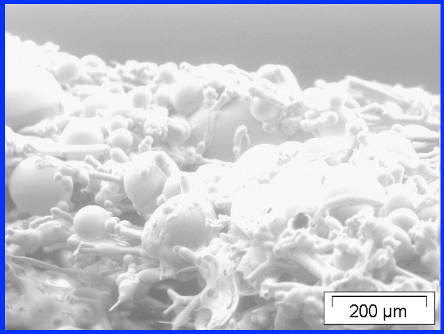

O(mm)

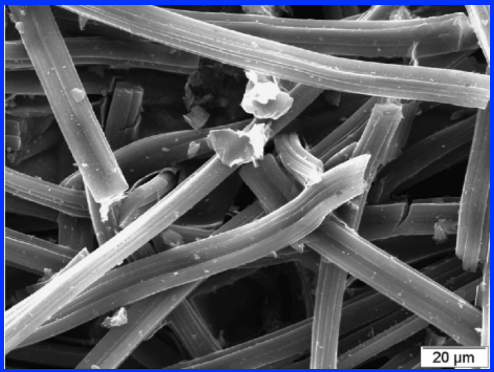

O(µm)

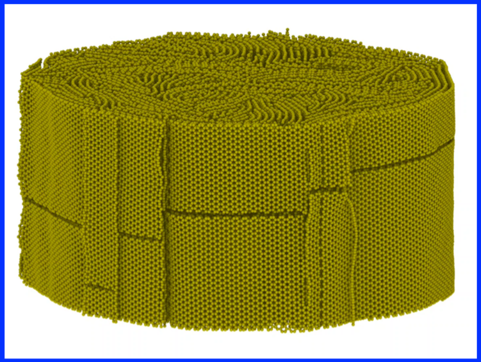

O(nm)

Movie courtesy: Linyuan (Mike) Shi, Arvind Srikanth, Marina Sessim, Michael Tonks, Simon Phillpot, *Materials Science and Engineering, U. of Florida (Feb 2019)*

Stardust Return Earth atmosphere entry (2006)

High-enthalpy environment during atmospheric entry

Return entry speed (Earth-atmosphere): 12.8 km/s

Stardust core

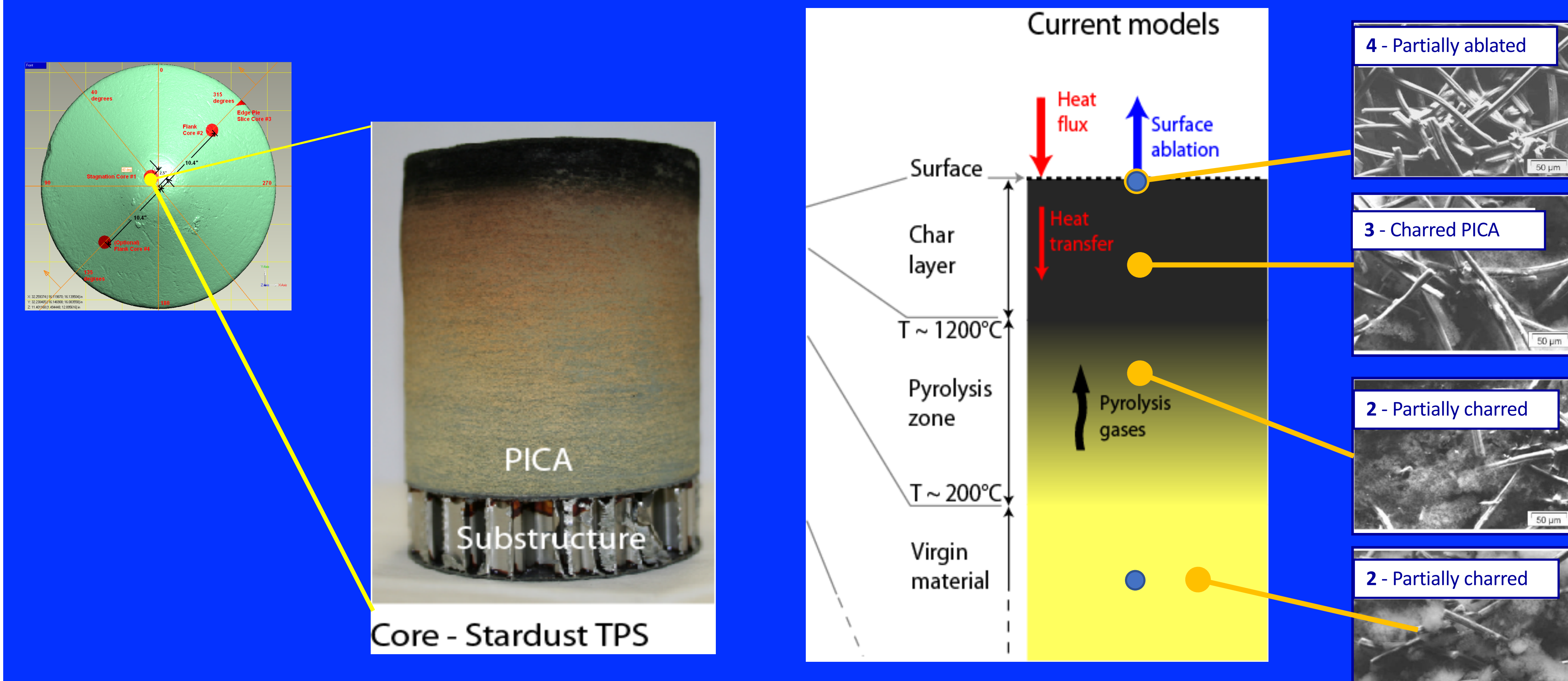

view at the macro-scale

(1) Stardust core image from M. Stackpoole *et al.*, Post-Flight Evaluation of Stardust Sample Return Capsule Forebody Heatshield Material, AIAA 2008-1202

SEM micrographs (1)

Microscopic Analysis of the TPS of Stardust

Flow regime in the pores of the material: from Knudsen to continuum

Knudsen number in the pores along the Stardust trajectory[1]

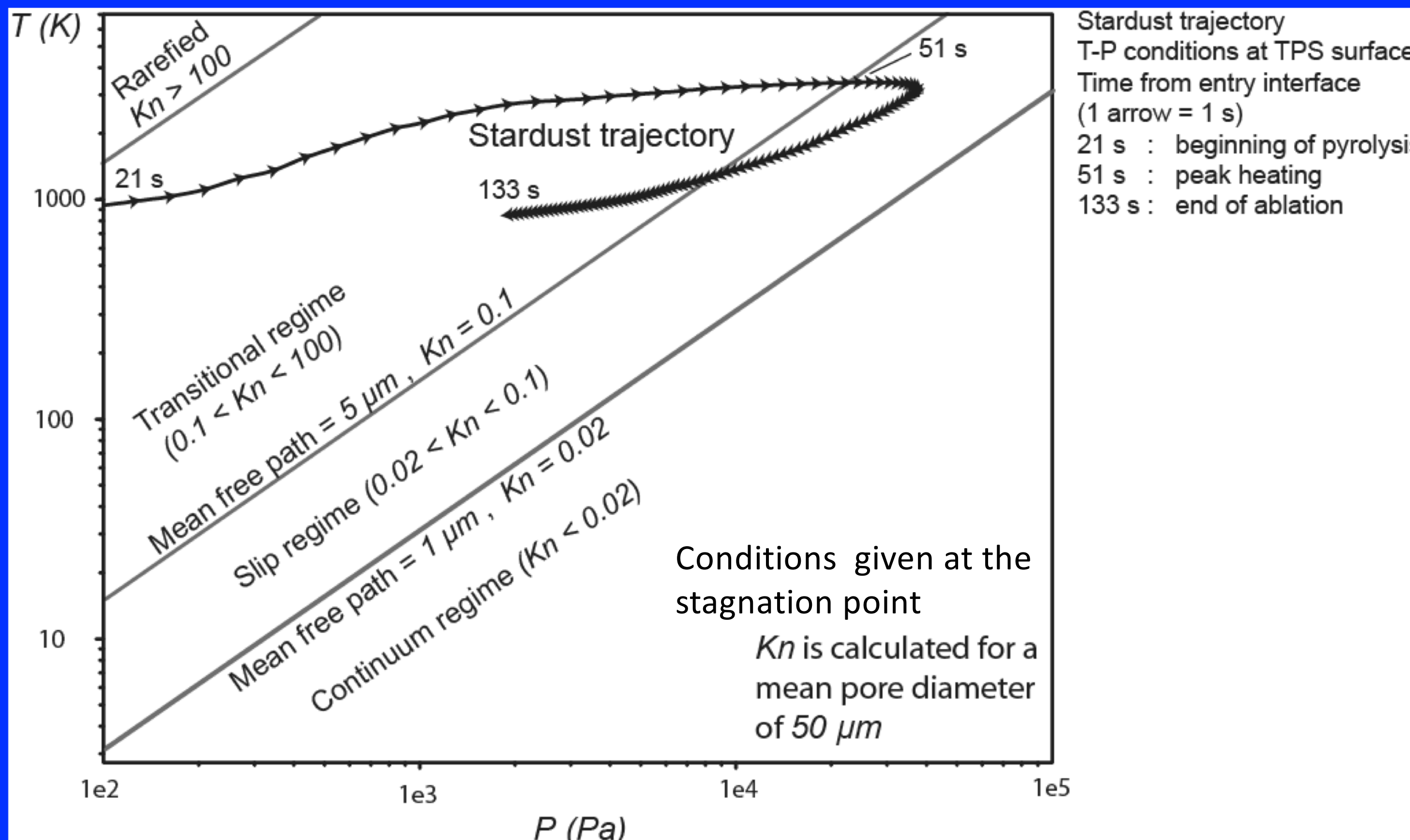

J. Lachaud, I. Cozmuta, N. N. Mansour. Multiscale approach to ablation modeling of phenolic impregnated carbon ablators. Journal of Spacecraft and Rockets, Vol. 47, No. 6, Nov.–Dec. 2010

Stardust post flight analysis (2008)

46th AIAA Aerospace Sciences Meeting and Exhibit
7 - 10 January 2008, Reno, Nevada

AIAA 2008-1202

Post-Flight Evaluation of Stardust Sample Return Capsule Forebody Heatshield Material

Mairead Stackpoole[*], Steve Sepka[†] and Ioana Cozmuta[‡]
ELORET Corporation, Sunnyvale, CA, 94086

Dean Kontinos[§]
Ames Research Center, Moffett Field, CA, 94035

Phenolic Impregnated Carbon Ablator (PICA) was developed at NASA Ames Research

For the near stagnation core, the model over predicts recession by 61 percent. For the flank core, the difference in the predicted recession values is 25 percent. The discrepancies at the flank core are of the same order as differences between calculation and arc-jet tests against which the model was calibrated.[5] The over-prediction at the near-stagnation core is not fully understood.

strength assessment of remaining virgin PICA, an emissivity profile, a chemical analysis profile, and a microstructural analysis. Results show good agreement in comparisons of experimental density profiles and profiles derived from FIAT and in recession comparisons from measured values and FIAT predictions for the flank core. In general, the PICA material examined in the cores is in good condition and intact. Impact damage is not evident, and the only degradation observed was that caused by heating on entry. A substantial amount of virgin PICA was present in all cores examined.

Have we reached the limitations of Kendall's model (used in current codes)?

Flight data: MEDLI's MISP plug

The heat shield of the The Mars Science Laboratory (MSL) was instrumented with a suite of sensors.

These provided for the first time flight data on PICA

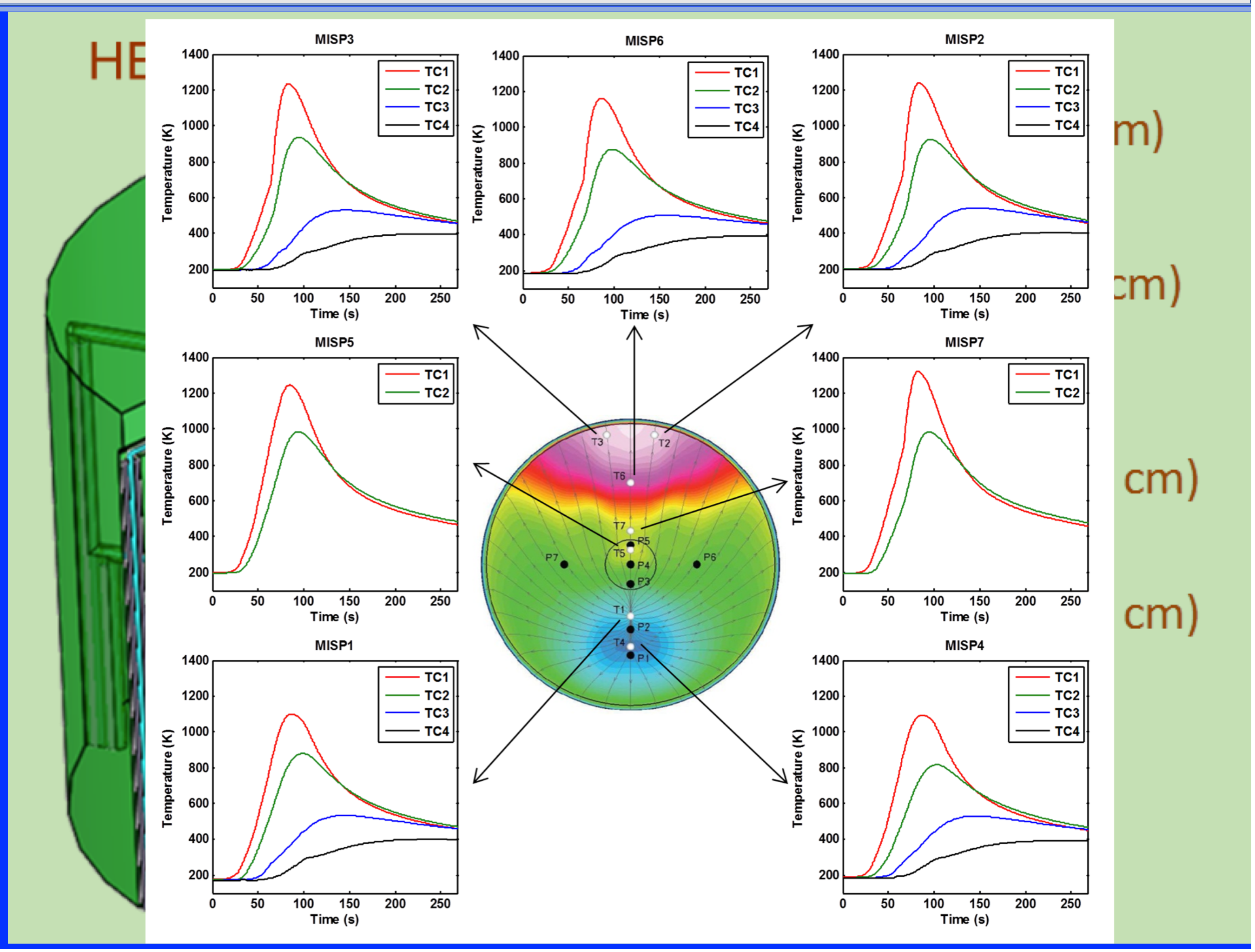

Bose et al. AIAA 2013-0908

Flight data: MEDLI

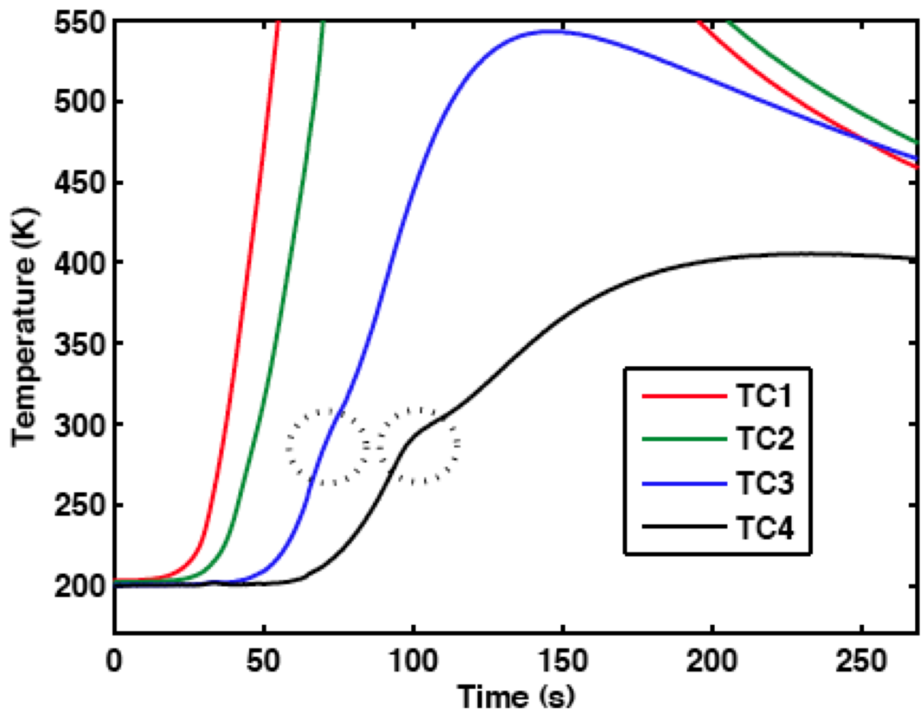

Figure 4. The "hump" observed in TC3 and TC4 data for plug 2 (seen also for other plugs).

Bose et al. AIAA 2013-0908

Performance of Current State Of the Art (Mahzari 2013)

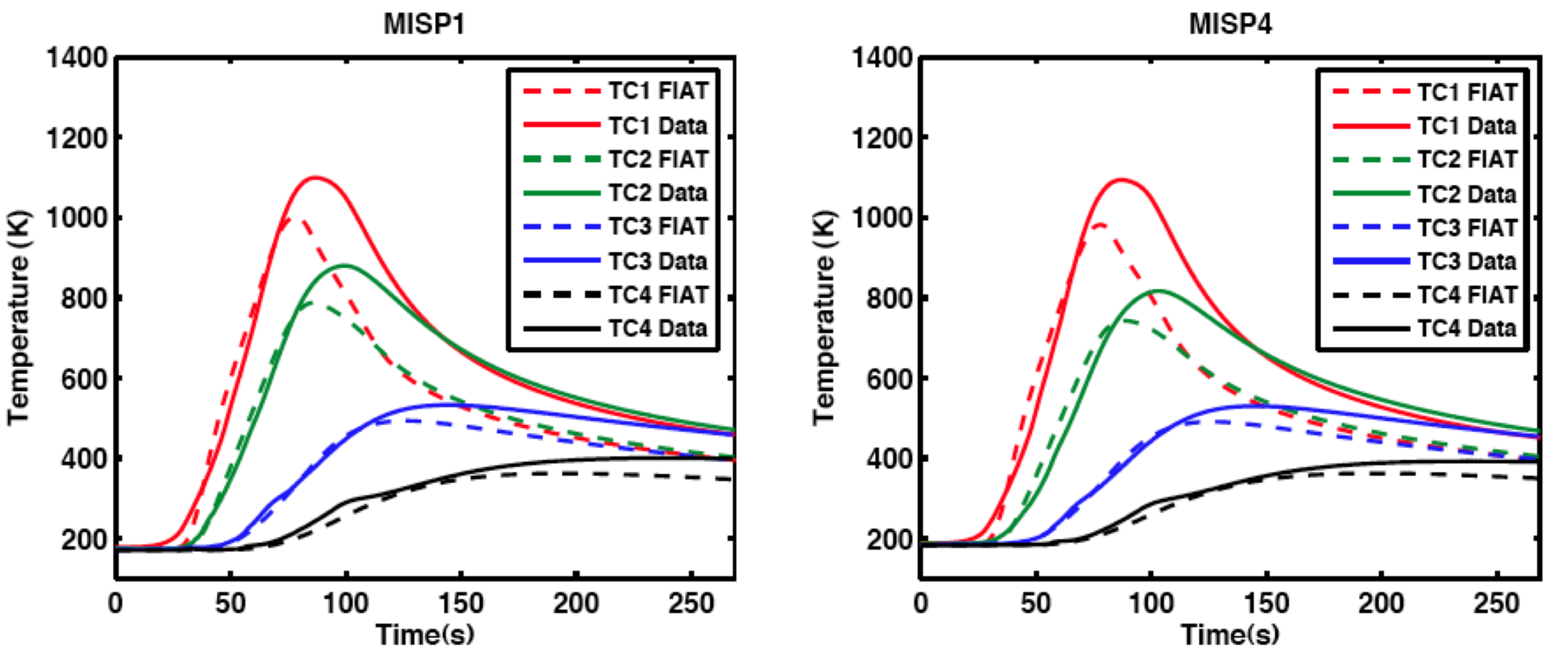

Figure 8. FIAT predictions compared with flight data for plugs 1 and 4.

Mahzari et al. AIAA 2013-0185

Performance of Current State Of the Art (Mahzari 2013)

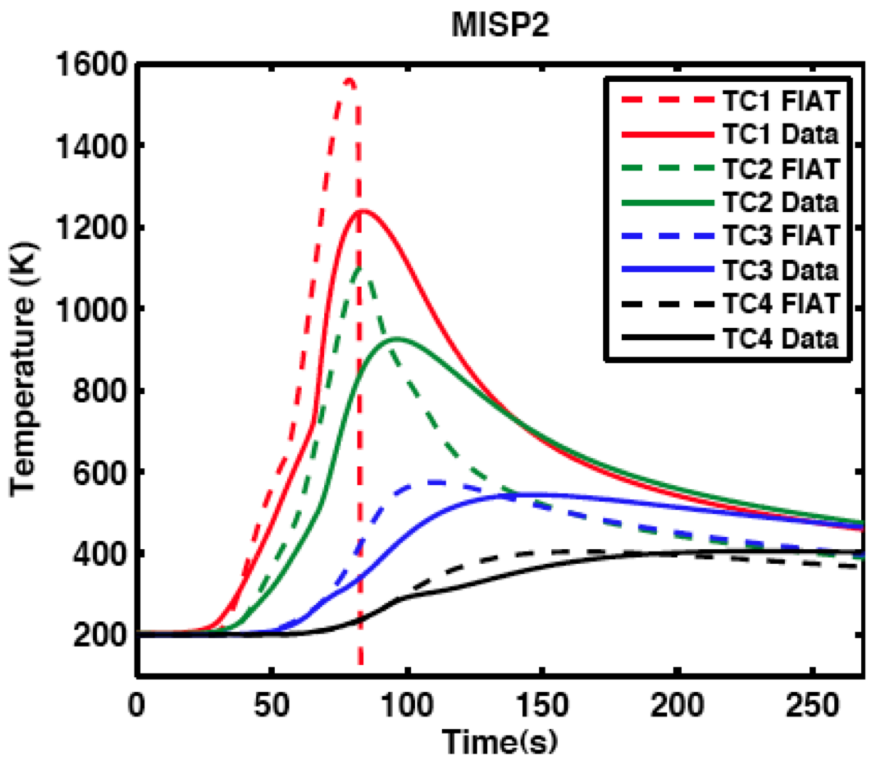

Figure 9. FIAT predictions compared with flight data for plugs 2 and 3.

Mahzari et al. AIAA 2013-0185

PMM: The four legged stool

- Experimental Validation Datasets
  - In house and via partnerships with Academia
- Microscale material model (PuMA)
  - Allows for interpretation of experimental data and construction of macroscale models
- Macroscale material model (PATO)
  - Reference standard Type 3 code for sensitivity analysis and limited engineering design
- Engineering response model (Icarus)
  - CFD integration and efficient engineering analysis

The "fifth" leg is to build a national/international community to address the current state and needs of ablation models

PMM Objective: high-fidelity material models

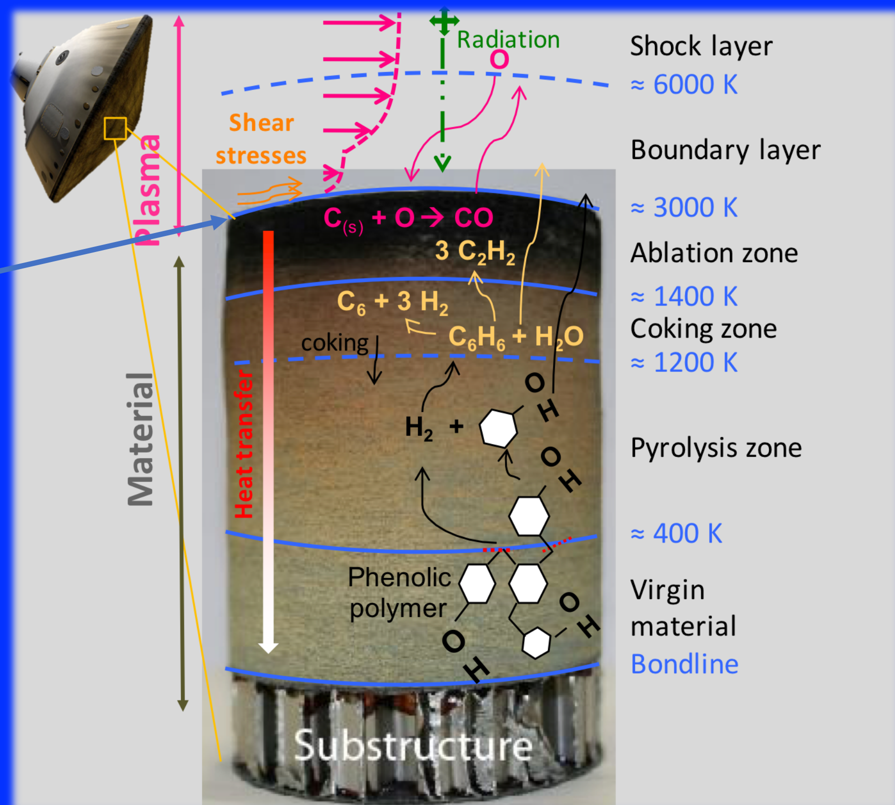

NuSil barrier T< 1000 K

Micrograph of Fiberform

Panerai et al., *J. Thermophys Heat Transfer* 28 (2014), 181-190

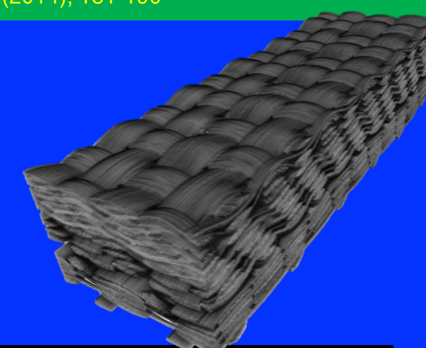

The microstructure of the material needs to enter into a macrostructure model, PICA ≠ woven materials

Building a model for PICA class

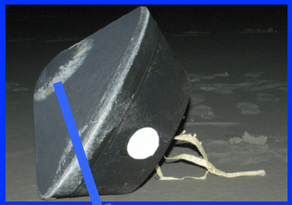

Core - Stardust TPS

Stardust core image from M. Stackpoole *et al.*, Post-Flight Evaluation of Stardust Sample Return Capsule Forebody Heatshield Material, AIAA 2008-1202

Before you do anything in ablation modeling you need:

0. Properties of the material: pyrolysis, conductivity, permeability, etc.
   a. Experimental data
      i. Pyrolysis experiments
      ii. Gas surface interactions data
      iii. Permeability
   b. Micro-computed tomography (microCT) of the material for bulk properties
      i. conductivity
      ii. permeability
      iii. tortuosity
1. Modeling at the macroscale
2. Material response codes
   1. PuMA
   2. PATO
3. Modeling spallation
4. Flow environment coupling

Building a model for PICA class

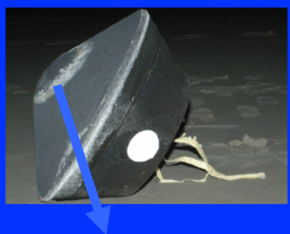

Core - Stardust TPS

Stardust core image from M. Stackpoole *et al.,* Post-Flight Evaluation of Stardust Sample Return Capsule Forebody Heatshield Material, AIAA 2008-1202

Before you do anything in ablation modeling you need:

0. Properties of the material: pyrolysis, conductivity, permeability, etc.
   a. Experimental data
      i. Pyrolysis experiments
      ii. Gas surface interactions data
      iii. Permeability
   b. Micro-computed tomography (microCT) of the material for bulk properties
      i. conductivity
      ii. permeability
      iii. tortuosity
1. Modeling at the macroscale
2. Material response codes
   1. PuMA
   2. PATO
3. Modeling spallation
4. Flow environment coupling

Building a model for porous materials(Lachaud et al. IJHMT 2017)

Volume Averaging the conservation equations for mass momentum and energy

Averaging volume: dV

Averaging volume on a phase:

$$dV_i = \int_{dV} \gamma_i dv \quad \text{where} \quad \gamma_i = \begin{cases} 1 & \text{for } i \in \text{ phase } i \\ 0 & \text{otherwise} \end{cases}$$

Volume fraction of a phase:

$$\epsilon_i = \frac{dV_i}{dV} \qquad \gamma_i = g/0, 1, 2, 3, ...$$

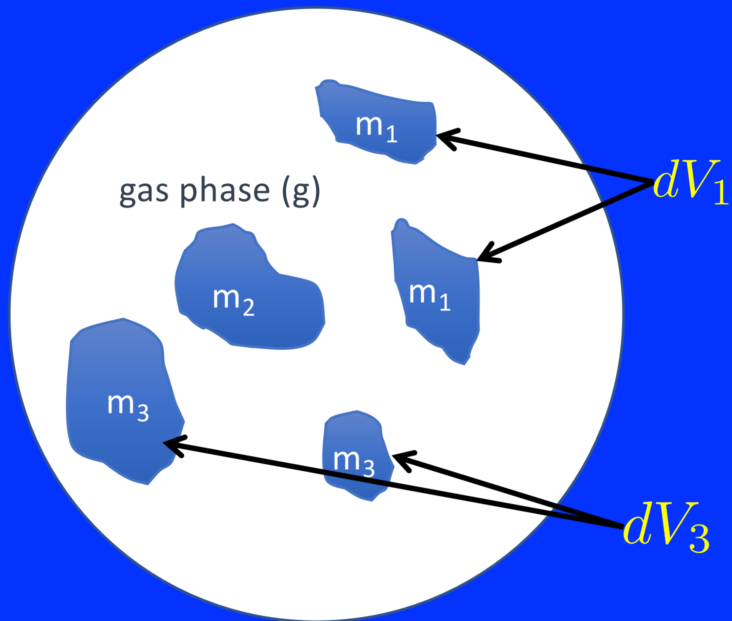

Lachaud et al. A generic local thermal equilibrium model for porous reactive materials submitted to high temperatures IJHMT 108 (2017) 1406–1417

Model development (Lachaud et al. IJHMT 2017)

A unified model multi-phase porous reactive materials subjected to high-temperature

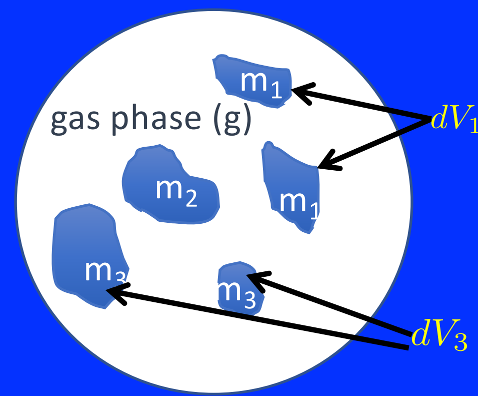

Hypotheses

- multi-phase reactive material
- multi-species reactive gas mixture
- local spatial deviations small
  - pore size small compared to the dimensions of the problem
  - pore-scale phenomena fast compared to large scale phenomena
    - ➢ pore-scale diffusion >> overall convection,
    - ➢ pore-scale diffusion >> reaction

Macroscopic intrinsic variables are local space average

$$\langle \rho \rangle_i = \frac{1}{dV_i} \int_{dV_i} \rho_i(v) dv$$

Extensive variables may be summed

$$\langle \rho \rangle = \sum_{i \in s} \epsilon_i \langle \rho \rangle_i + (1 - \epsilon_i) \langle \rho \rangle_g$$

For simplicity of the notation the averaging symbol is dropped unless it is needed for clarity

Lachaud et al. A generic local thermal equilibrium model for porous reactive materials submitted to high temperatures IJHMT 108 (2017) 1406–1417

Model development (Lachaud et al. IJHMT 2017)

Multi-phase multi-mechanism pyrolysis model

- multi-phase reactive material (i=[0,N_p])
- multi-mechanism pyrolysis model (j=[1,R_i])
- multi-specie/elements production (k=[1,N_g])

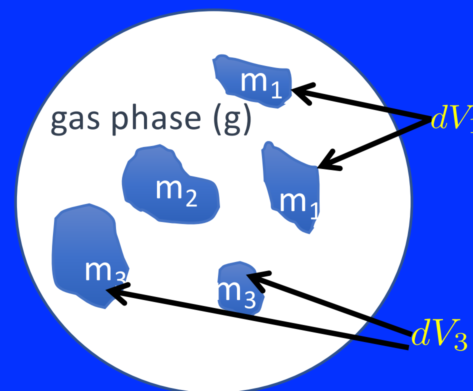

$$R_{ij} \rightarrow \sum_{k\in[1,N_g]} \zeta_{ijk} A_k \qquad \forall i \in [1, N_p],\ \forall j \in [1, R_i]$$

Stoichiometric coefficients

Advancement of reaction j in phase i (Arrhenius)

$$\frac{\partial_t \chi_{ij}}{(1-\chi_{ij})^{m_j}} = T^{n_j} \mathcal{A}_j \exp\left(-\frac{E_j}{\mathcal{R}T}\right)$$

Production of species k

$$\pi_k = \sum_{i\in[1,N_p]} \sum_{j\in[1,N_i]} \zeta_{ijk} \epsilon_{i,0} \rho_{i,0} F_{ij} \partial_t \chi_{ij}$$

Decomposing phenolic single solid phase

$$\text{Solid}\begin{cases} R_1 \xrightarrow{F_1=0.06} 0.62\mathrm{H_2O} + 0.38\mathrm{CO} \\ R_2 \xrightarrow{F_2=0.01} 0.69\mathrm{CO_2} + 0.21\mathrm{C_3H_8O_{,1}} + 0.09\mathrm{C_3H_8O_{,2}} \\ R_3 \xrightarrow{F_3=0.20} 0.42\mathrm{H_2O} + 0.06\mathrm{CO_2} + 0.15\mathrm{C_6H_5OH} + 0.34\mathrm{C_7H_8O} + 0.03\mathrm{C_8H_{10}} \\ R_4 \xrightarrow{F_4=0.19} 0.67\mathrm{CO} + 0.27\mathrm{CH_4} + 0.03\mathrm{C_6H_6} + 0.04\mathrm{C_7H_8} \\ R_5 \xrightarrow{F_5=0.03} 1.00\mathrm{H_2} \\ R_6 \xrightarrow{F_6=0.06} 0.19\mathrm{H_2} + 0.81\mathrm{CO} \\ \text{Char} \end{cases}$$

Mass spectrometry measurements (Bessire & Minton 2017)

TECHNICAL APPROACH

- Novel application of mass spectrometric techniques in vacuum, to obtain *in situ* experimental data for decomposing polymers.
- Ability to control sample heating rate from ambient to >2200 K.
- Molar yields, mass yields, and TGA of pyrolysis gases are collected as a function of temperature and heating rate, for phenolic resin-based TPS materials.

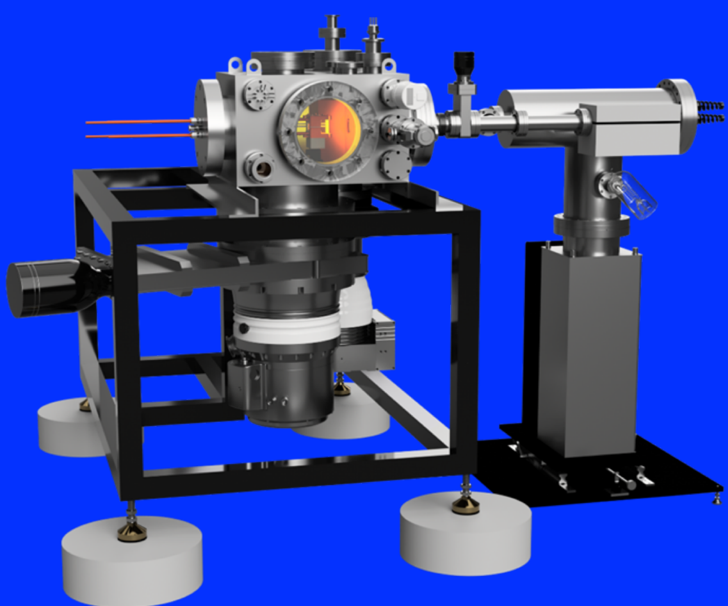

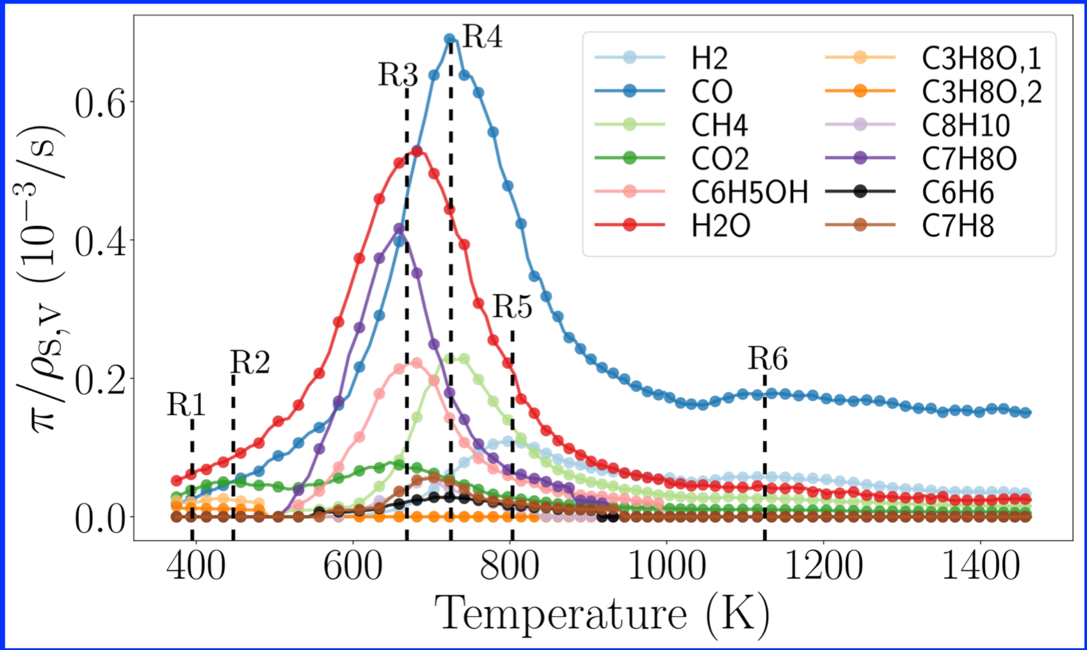

Bessire & Minton ACS Appl. Mater. Interfaces 2017, 9, 21422–21437

Methodology (Torres et al. 2019)

Coupling material solver with optimizer.

- More details about the optimizer are described in the talk of Francisco Torres

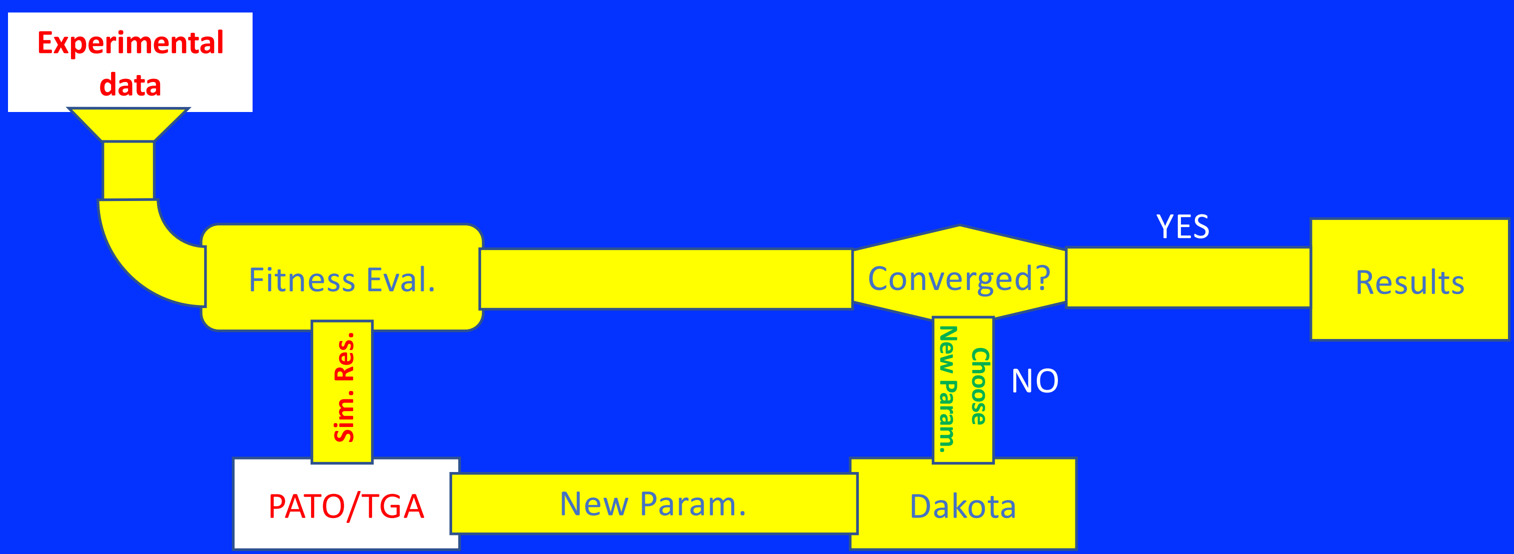

Material solver: Porous Media Analysis Toolbox (PATO, NASA)

Optimizer: Dakota (Sandia Laboratories)

Francisco Torres Herrador, *et al.* “A high heating rate pyrolysis model for the Phenolic Impregnated Carbon Ablator (PICA) based on mass spectroscopy experiments,” submitted for pub. 2019

Results – Species model (Torres et al. 2019)

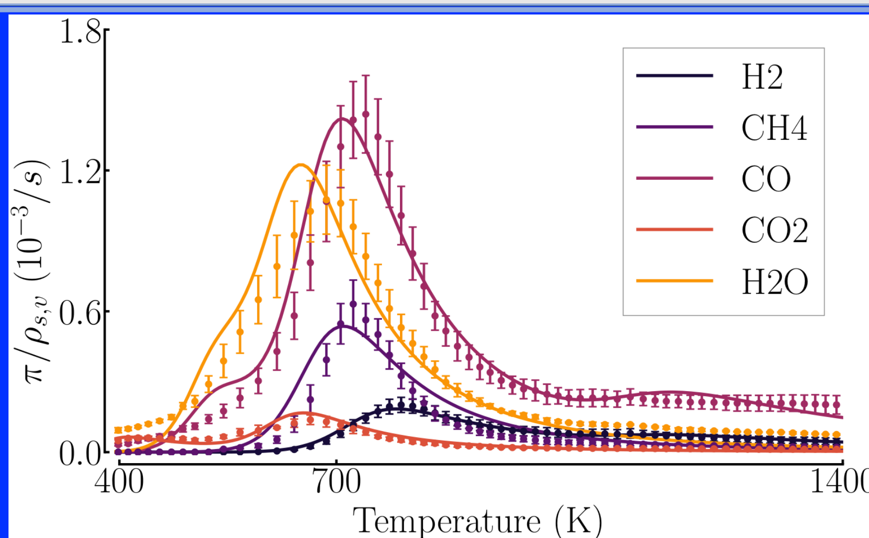

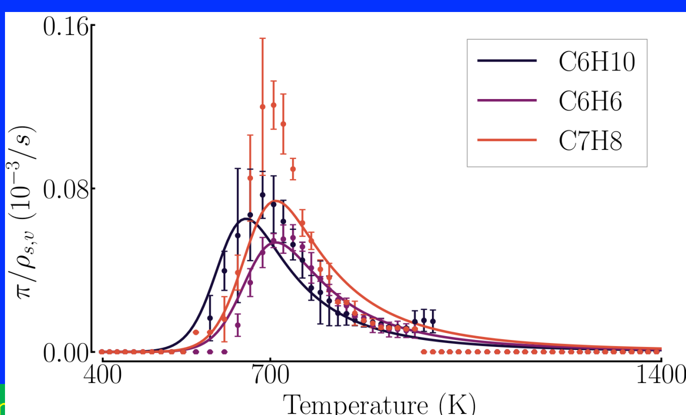

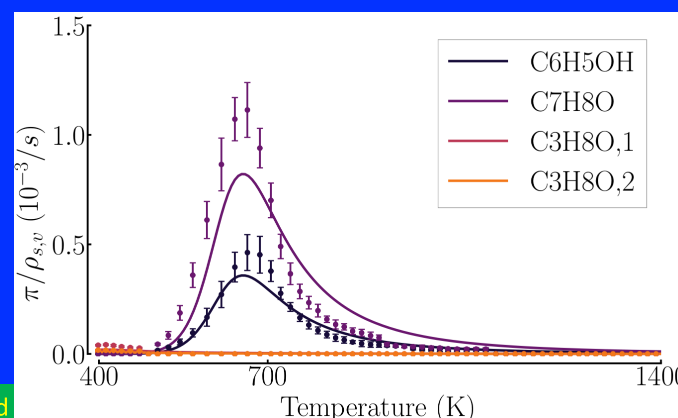

Fran… …or the Phenolic Impregnated … …submitted for pub. 2019

Results – TGA

Production of species k

$$\pi_k = \sum_{i\in[1,N_p]} \sum_{j\in[1,N_{R_i}]} \zeta_{ijk}\epsilon_{i,0}\rho_{i,0}F_{ij}\partial_t\chi_{ij}$$

For a single phase (phenolic) i=1, we have

$$\pi_k = \sum_{j\in[1,N_{R_1}]} \zeta_{1jk}\epsilon_{1,0}\rho_{1,0}F_{1j}\partial_t\chi_{1j}$$

$$\frac{\pi_k}{\epsilon_{1,0}\rho_{1,0}} = \sum_{j\in[1,N_{R_1}]} \zeta_{1jk}F_{1j}\partial_T\chi_{1j}(\partial_T/\partial_t)$$

$$\ldots$$

Francisco Torres Herrador, *et al.* "A high heating rate pyrolysis model for the Phenolic Impregnated Carbon Ablator (PICA) based on mass spectroscopy experiments," submitted for pub. 2019

Results – Species model (Torres et al. 2019)

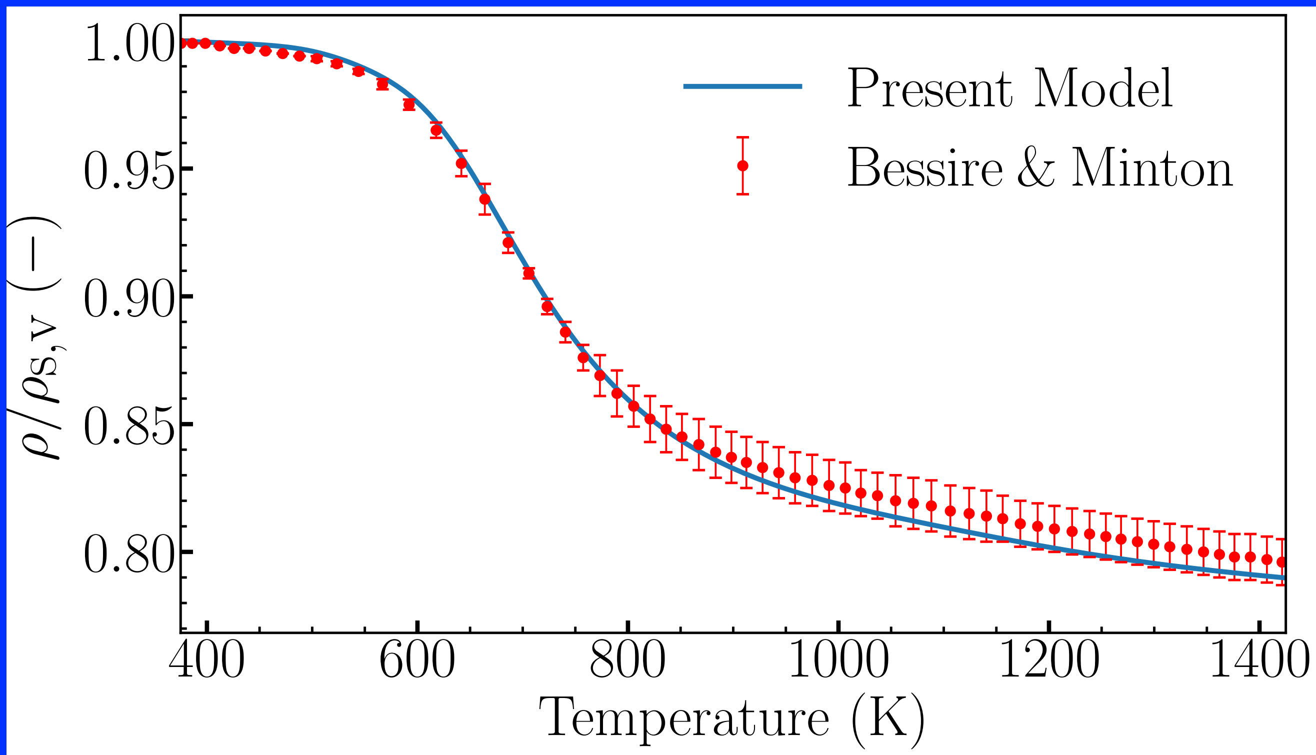

Francisco Torres Herrador, *et al.* "A high heating rate pyrolysis model for the Phenolic Impregnated Carbon Ablator (PICA) based on mass spectroscopy experiments," submitted for pub. 2019

Building a model for PICA class

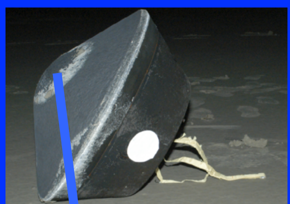

Core - Stardust TPS

Before you do anything in ablation modeling you need:

0. Properties of the material: pyrolysis, conductivity, permeability, etc.
   a. Experimental data
      i. Pyrolysis experiments
      ii. Gas surface interactions data
      iii. Permeability
   b. Micro computed-tomography (microCT) of the material for bulk properties
      i. conductivity
      ii. permeability
      iii. tortuosity
1. Modeling at the macroscale
2. Material response codes
   1. PuMA
   2. PATO
3. Modeling spallation
4. Flow environment coupling

Stardust core image from M. Stackpoole *et al.,* Post-Flight Evaluation of Stardust Sample Return Capsule Forebody Heatshield Material, AIAA 2008-1202

Conductivity from tomography

The summation rule over phases works for extensive variable such as volume, mass and energy, for example:

$$\frac{\langle m \rangle}{dV} = \langle \rho \rangle = \sum_{i \in [0, N_p]} \frac{m_i}{dV} = \sum_{i \in [0, N_p]} \frac{m_i}{dV_i} \frac{dV_i}{dV} = \sum_{i \in [0, N_p]} \epsilon_i \langle \rho_i \rangle$$

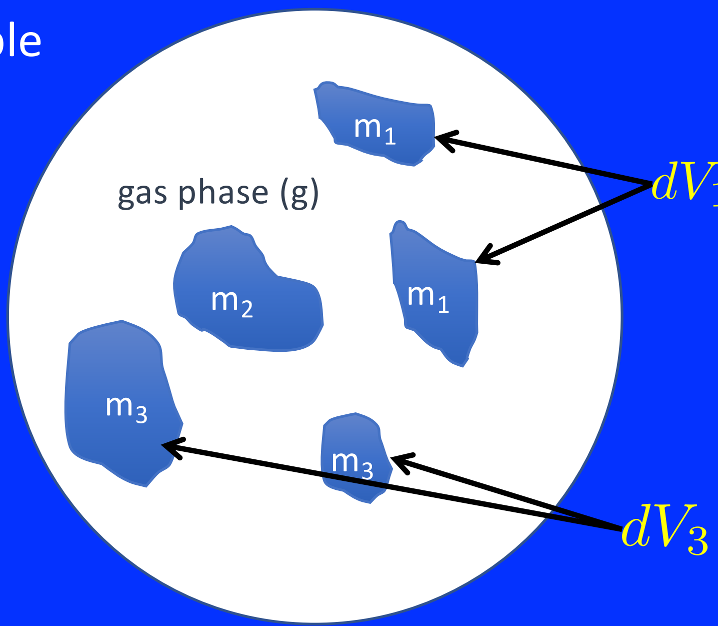

But does not work for intensive variable. It also does not work for properties. For example average the conductivity over the integration volume:

$$\langle k \rangle \neq \sum_{i \in [0, N_p]} \langle \epsilon_i \rangle \langle k_i \rangle$$

For effective properties at the macroscale, we resort to computing them by upscaling simulations on micro computed tomography 3D images of the material.

What is micro-Computed Tomography or micro-CT?

Multiple Angles

micro-CT: how it works

- 3D image quality depends on:
  - 2D image quality
  - Number of projections
  - Angular range of projections
  - Reconstruction algorithm

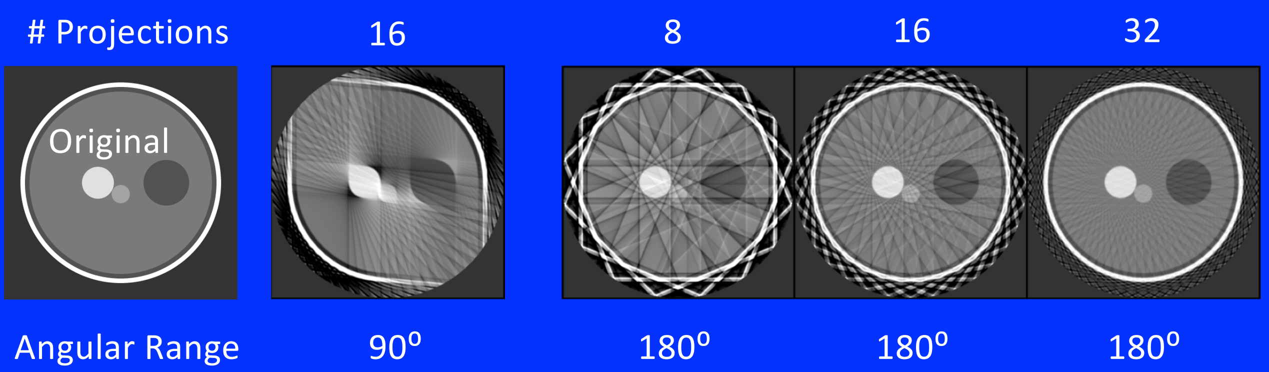

Tomography Experimental Setup

Collect X-ray images of the sample as you rotate it through 180 degrees

Use this series of images to "reconstruct" the 3D object

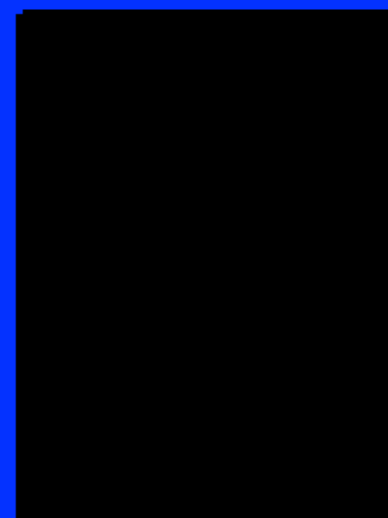

Penetrating Power

Multiple Angles

How bright are synchrotrons?

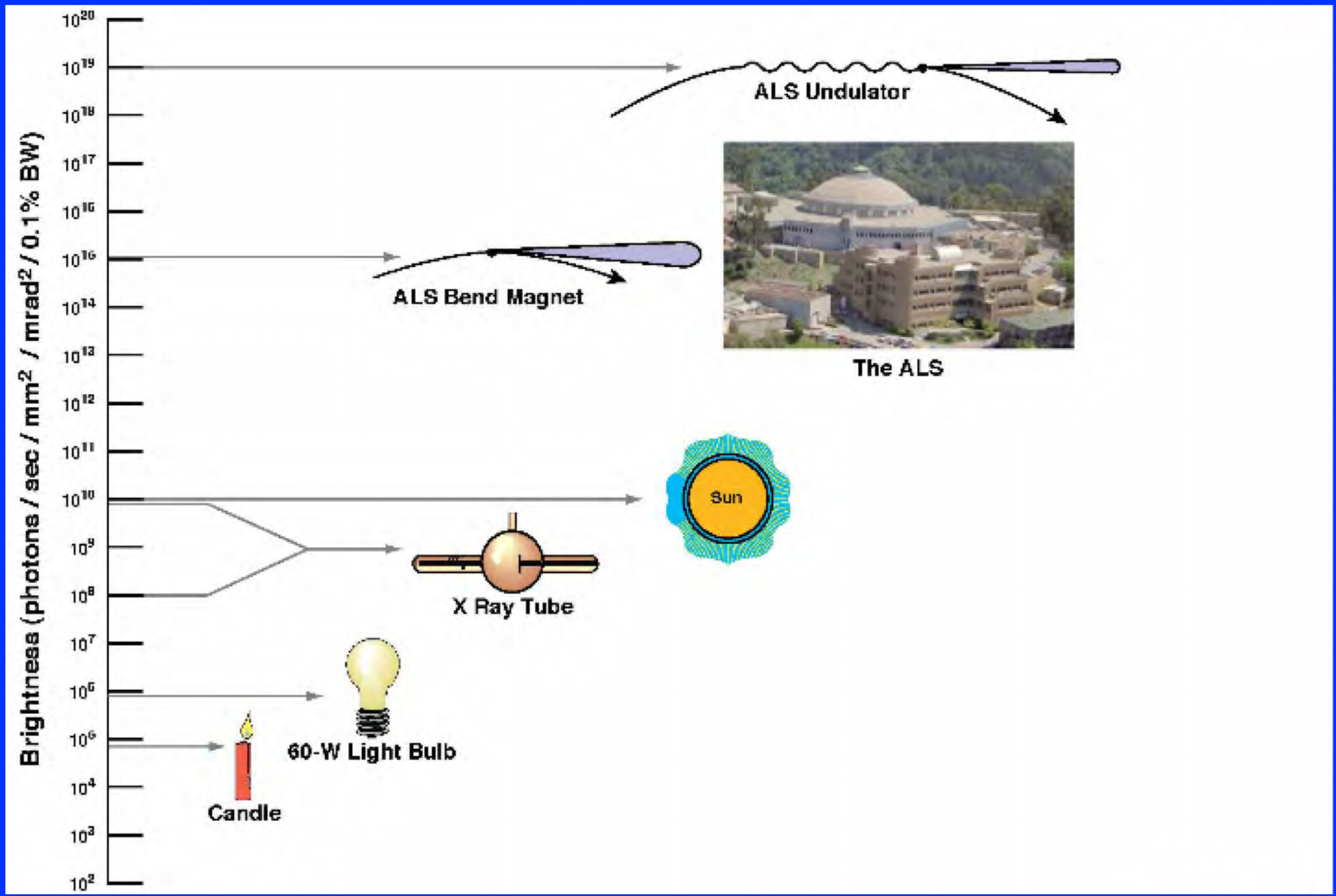

Synchrotron Micro-tomography at the ALS

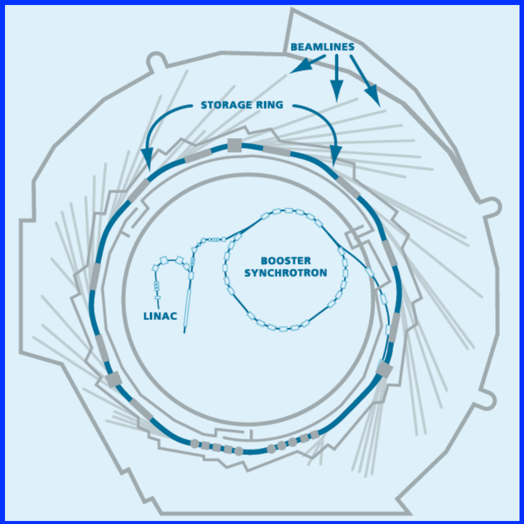

Why synchrotron micro-CT?

- Resolves 3D microstructure
- Provides high quality imaging
- Flexibility in samples dimensions and resolution
- Allows for in-situ experiments (tensile loads, high temperatures, reactive flows, etc.)

Inside the ALS

8.3.2 Tomography Beam line (Barnard 2016)

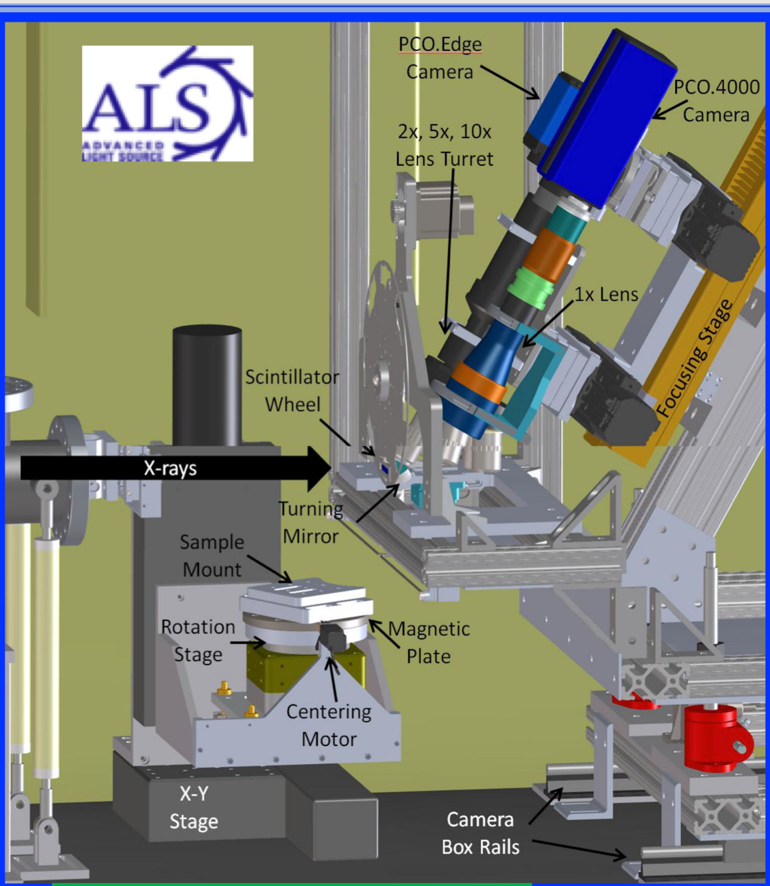

MacDowell et al., Proc. of SPIE Vol. 8506, 2012

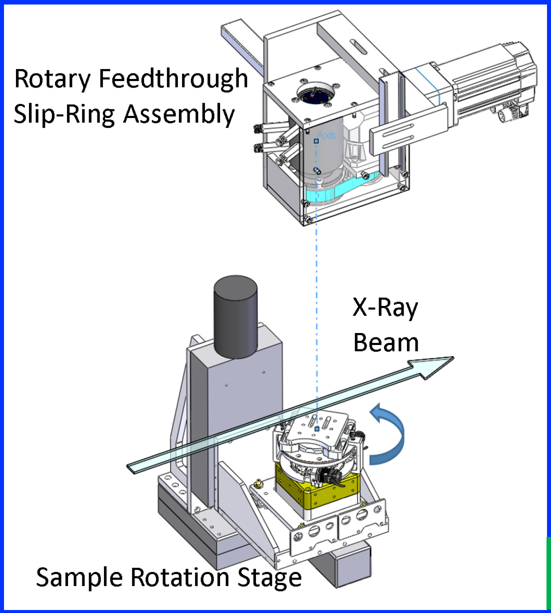

Barnard, H. et al. Proc. SPIE, Vol. 9967 (2016)

- Hard X-ray microtomography
- A monochromator selects the specific X-ray wavelength (energy operating range is 6-46 keV, plus white light is allowed)
- The sample is mounted on a rotating stage
- A scintillator converts X-rays into visible light
- The scintillator is imaged by a camera, through magnifying lenses

Tomography reconstruction

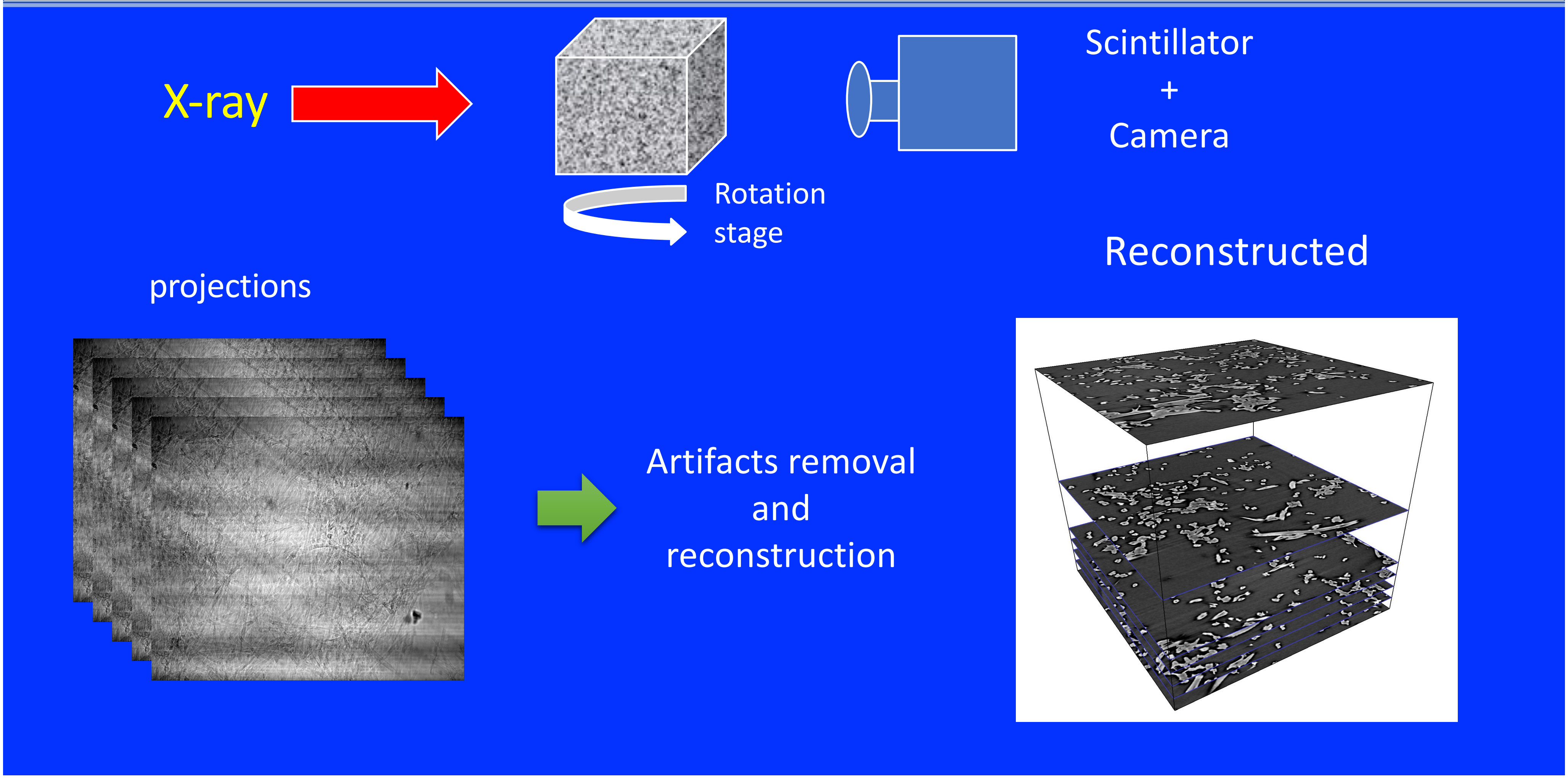

Picking the threshold

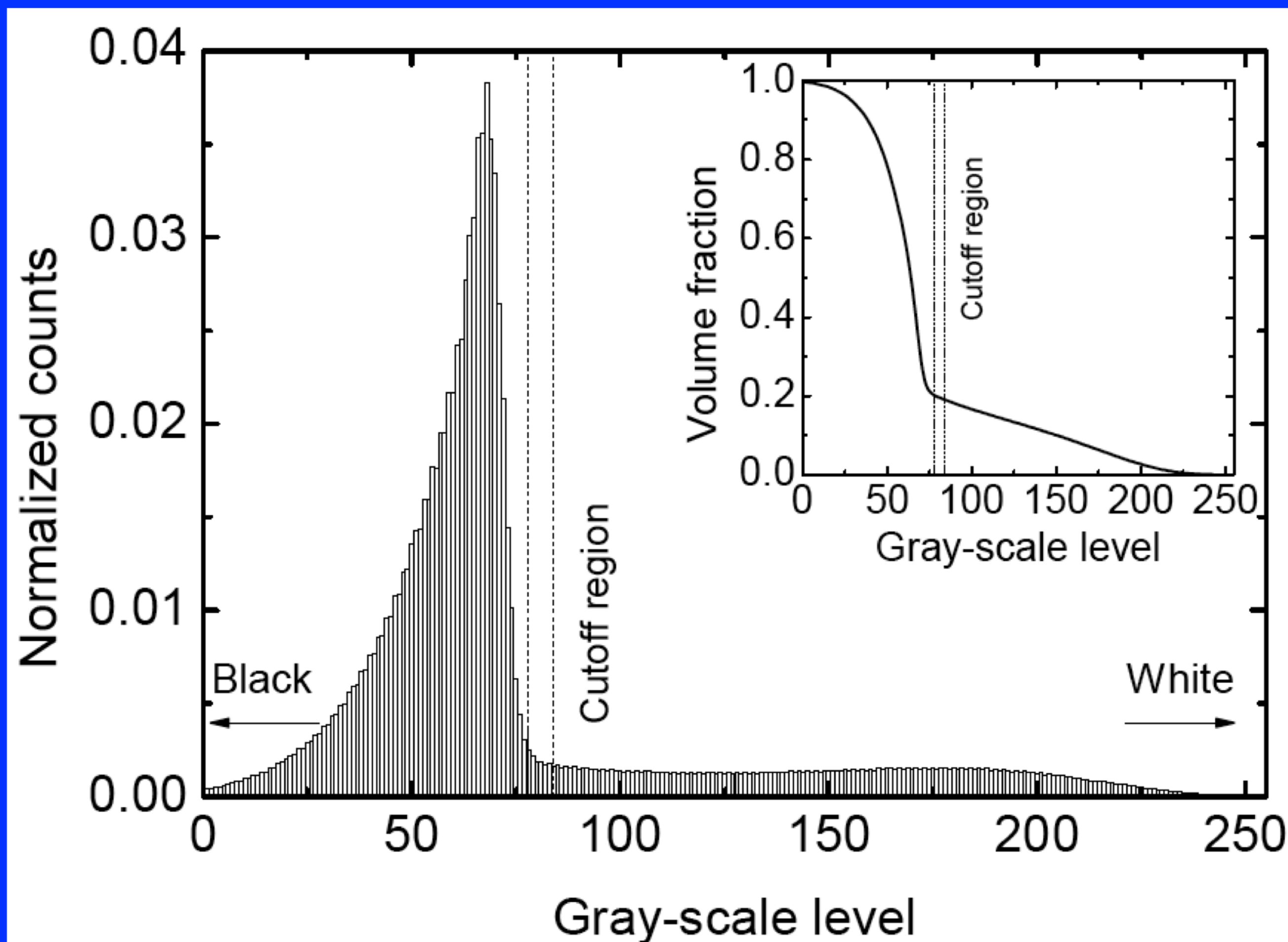

Post Processed images

Tomography of felt

Tomographic imagery of parachute cloth (Panerai 2017)

Synchrotron micro-tomography setup at Berkeley Lab

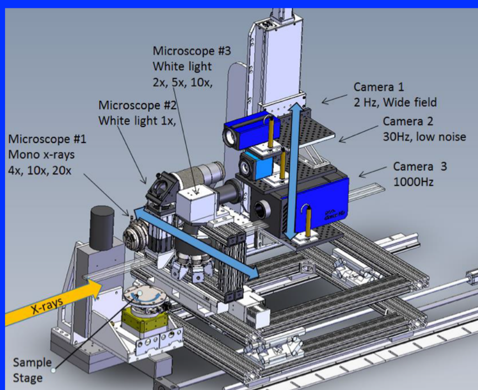

Setup for in-situ imaging of fabrics under tension:

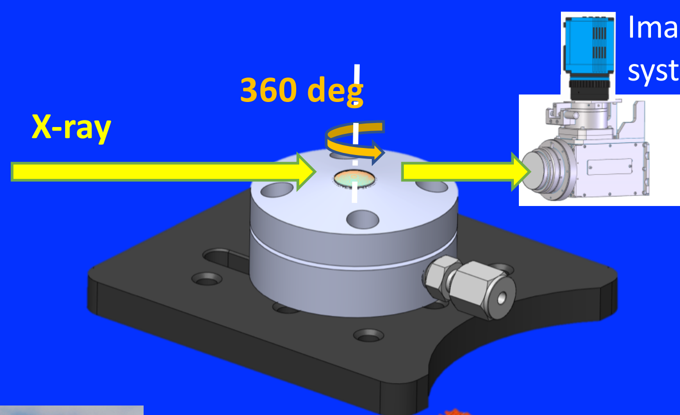

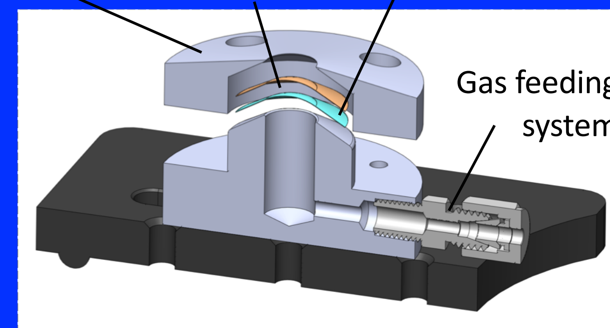

Section view

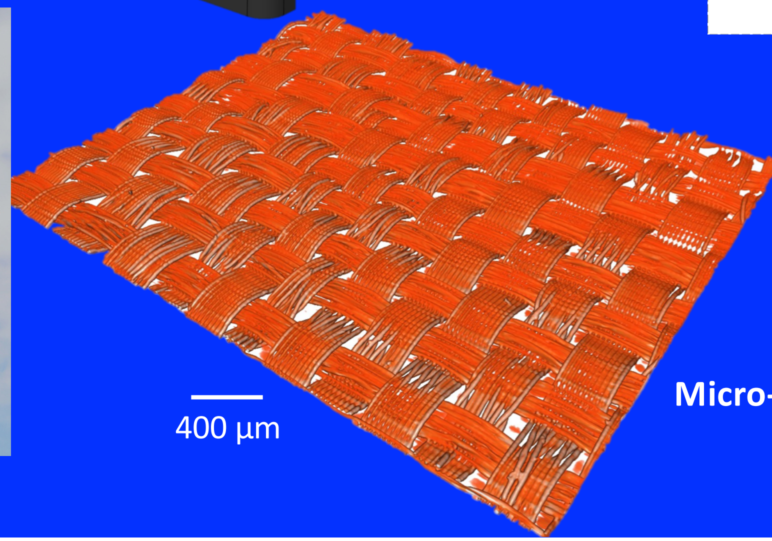

Micro-tomography of Nylon cloth

Direct numerical simulations from micro-CT scans

Micro-CT provides a digitized image of the material at the micro-scale

- The cut-off or level-set value determines interfaces between phases

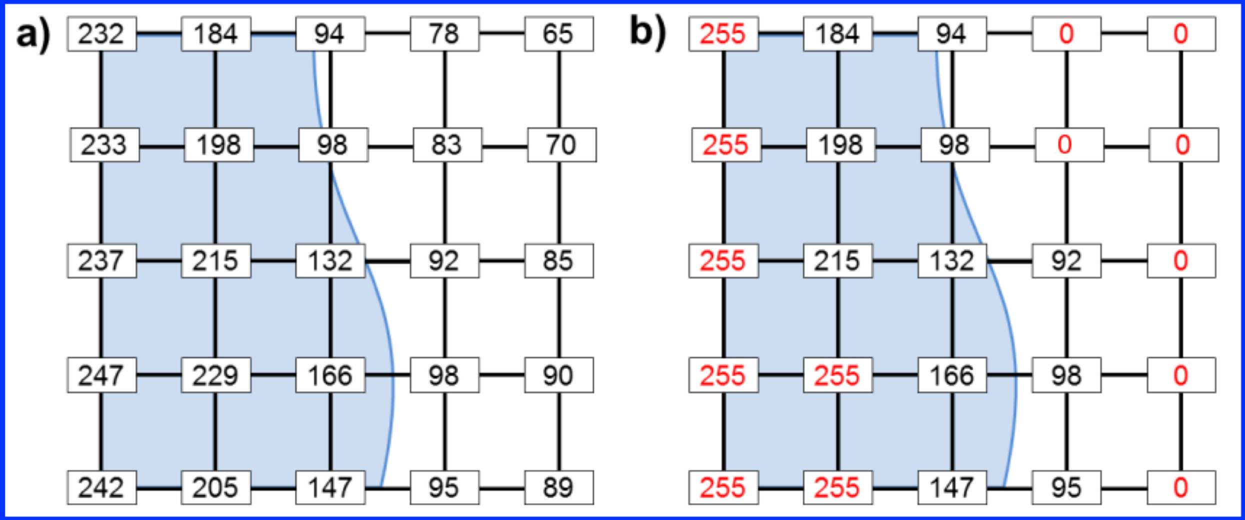

Having a digitized 3D image enables computing properties at the macro-scale from proteies at the micro-phase scale.

Effective conductivity at the macro-scale

At the micro-scale, we have

$$-q_i = kT_{,i}$$

Volume average over the macro-scale [d_x x d_y], we get

$$-\langle q \rangle_i = \langle kT_{,i} \rangle$$

$$\approx \langle k \rangle_{i1} \frac{\langle T \rangle_2 - \langle T \rangle_1}{d_x}$$

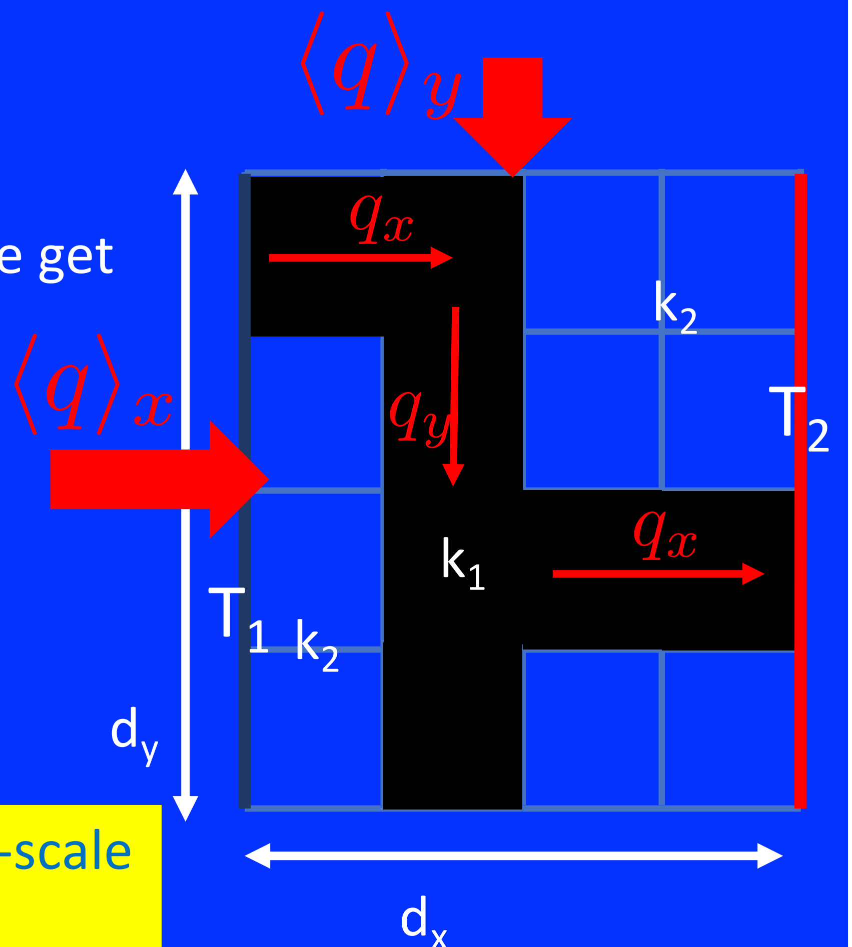

Strategy: Direct Numerical Solution at the micro-scale over a macro-scale averaging volume

Numerical formulation

Governing equations in dimensional coordinate

$$\frac{\partial}{\partial x_i^*}\left(k^*\frac{\partial T^*}{\partial x_i^*}\right) = 0$$

$$T^* = T_1^* \text{ at } x_l^* = 0$$

$$T^* = T_2^* \text{ at } x_l^* = d_l$$

Non-dimensionalize using

$$T = \frac{T^* - T_1^*}{T_2^* - T_1^*}$$

$$x_\alpha = \frac{x_\alpha^*}{d_\alpha} \qquad \text{for } \alpha = 1, 2, 3$$

we get,

$$\frac{\partial}{\partial x_i}\left(k\frac{\partial T}{\partial x_i}\right) = 0$$

$$T = 0 \text{ at } x_1 = 0$$

$$T = 1 \text{ at } x_1 = 1$$

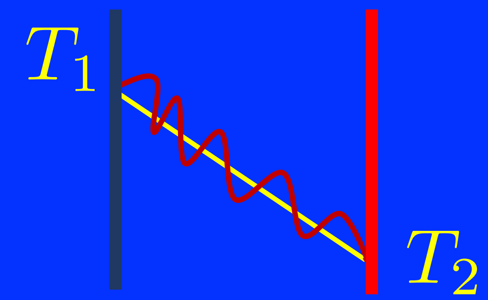

Homogenization, set. $T = \langle T \rangle + U$ where, $\langle U \rangle = 0$, and $\langle T \rangle$ satisfies the analytical solution at the macroscale

Numerical formulation

Using finite volume method and imposing continuity of temperature and heat flux at the interface between grids, after three pages of algebra you get:

$$
\frac{1}{h^2}\left(U_{i+1,j,k}+U_{i-1,j,k}\right)-2\frac{U_{i,j,k}}{h^2}-\frac{1}{2h}\left(J_{i+1/2,j,k}+J_{i-1/2,j,k}\right)
+\frac{1}{h^2}\left(U_{i,j+1,k}+U_{i,j-1,k}\right)-2\frac{U_{i,j,k}}{h^2}-\frac{1}{2h}\left(J_{i,j+1/2,k}+J_{i,j-1/2,k}\right)
+\frac{1}{h^2}\left(U_{i,j,k+1}+U_{i,j,k-1}\right)-2\frac{U_{i,j,k}}{h^2}-\frac{1}{2h}\left(J_{i,j,k+1/2}+J_{i,j,k-1/2}\right)=0
$$

$U_{i,j}$ is the homogenized temperature field and

$J_{i,j}$ are jump conditions at the interface

The system is then solved using a fast iterative scheme

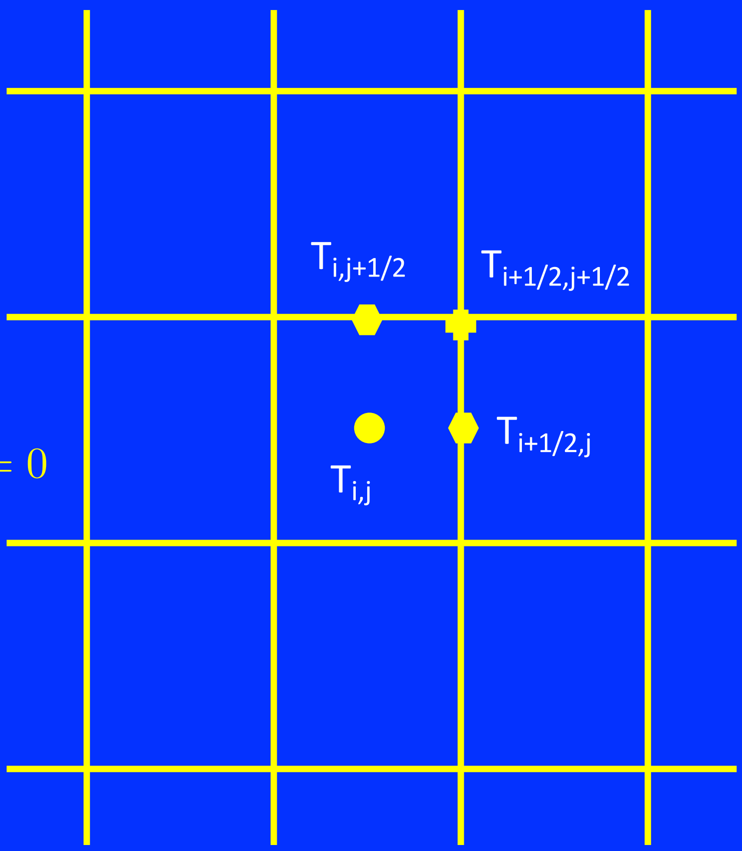

Effect of water on FiberForm Conductivity

$C+CO_2$	$C+H_2O+CO_2$	$C+ice+CO_2$	$C+H_2O$	$C+ice$

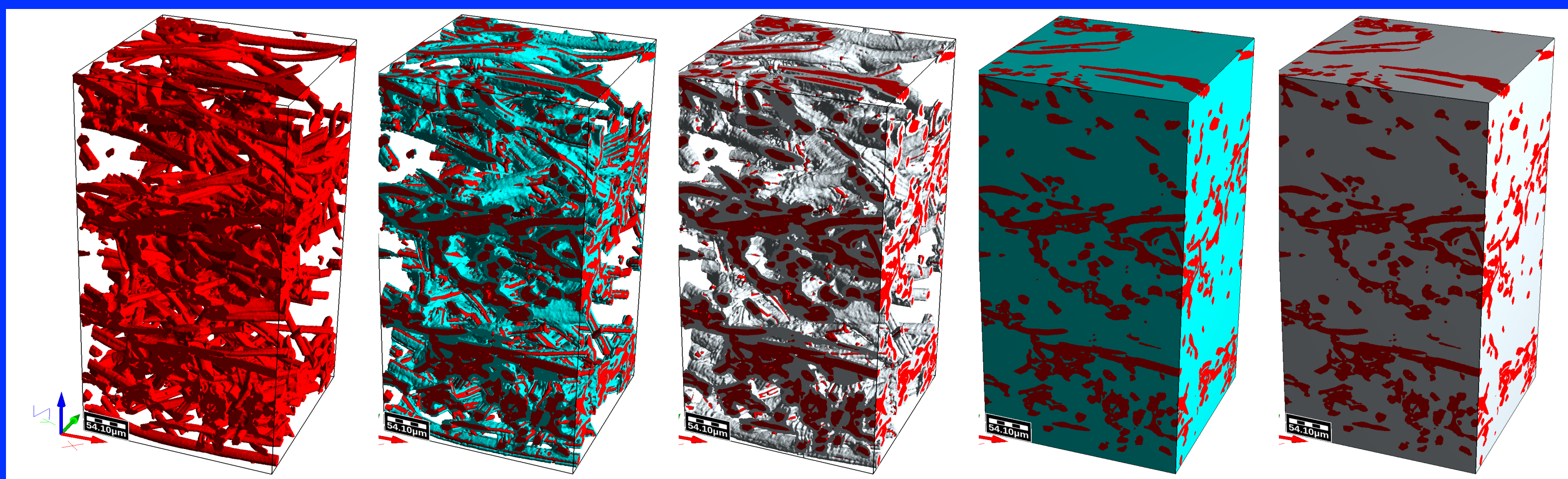

k_{eff}	$k_{eff} \times 1.005$	$k_{eff} \times 1.51$	$k_{eff} \times 3.13$	$k_{eff} \times 8.40$

Building a model for PICA class

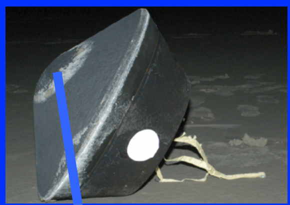

Core - Stardust TPS

Stardust core image from M. Stackpoole *et al.*, Post-Flight Evaluation of Stardust Sample Return Capsule Forebody Heatshield Material, AIAA 2008-1202

Before you do anything in ablation modeling you need:

0. Properties of the material: pyrolysis, conductivity, permeability, etc.
   a. Experimental data
      i. Pyrolysis experiments
      ii. Gas surface interactions data
      iii. Permeability
   b. Micro-computed tomography (microCT) of the material for bulk properties
      i. conductivity
      ii. permeability
      iii. tortuosity
1. Modeling at the macroscale
2. Material response codes
   1. PuMA
   2. PATO
3. Pyrolysis-ablation coupling
4. Flow environment coupling

Experiments: Permeability (Panerai et al. 2016)

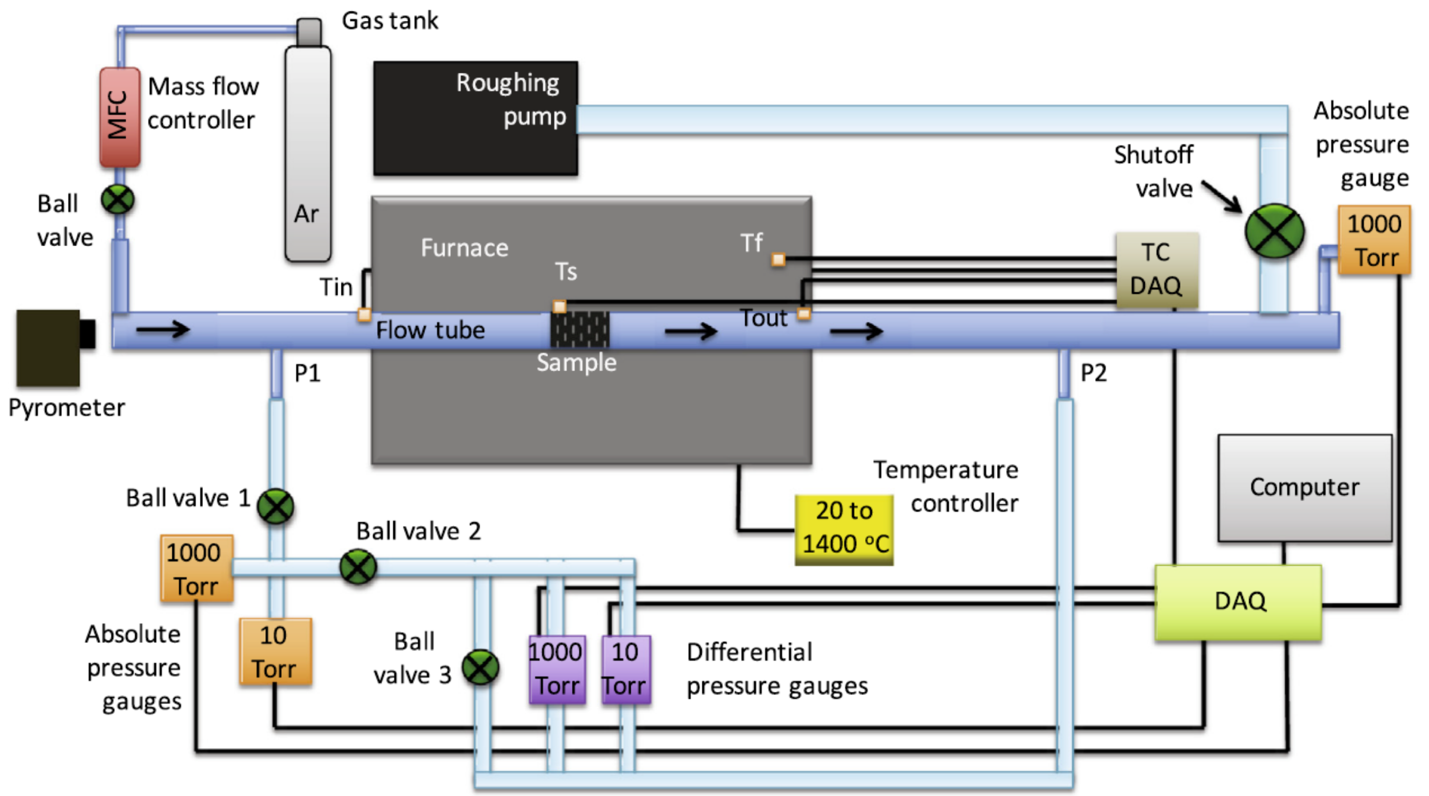

Fig. 2. Schematic of flow-tube setup at SRI International.

Panerai et al., *Int J Heat Mass Transfer* 101 (2016) 267–273

Experiments: Permeability (Panerai et al. 2016)

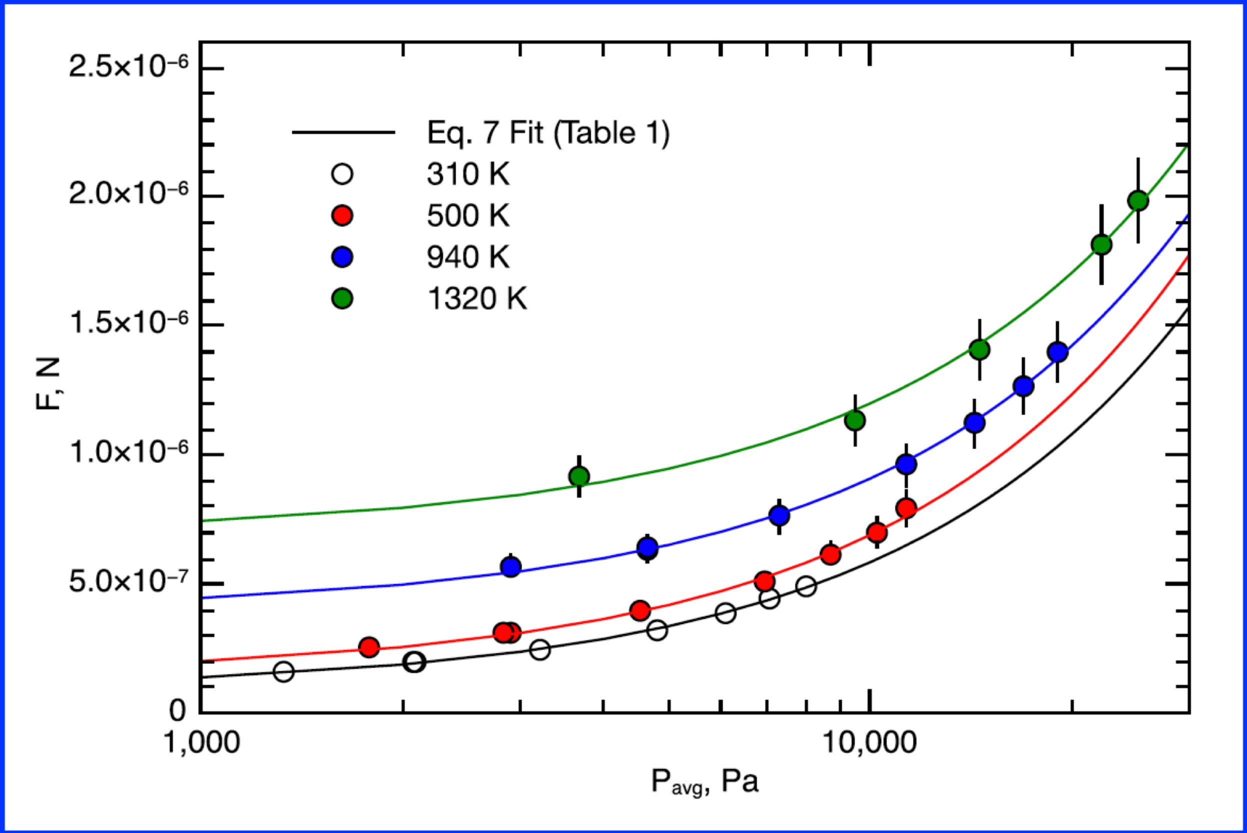

F vs average pressure. F is the resistive force, and d F/d P_{avg} is K_o, the permeability

Panerai et al., *Int J Heat Mass Transfer* 101 (2016) 267–273

Direct simulation Monte Carlo (Borner et al. 2017)

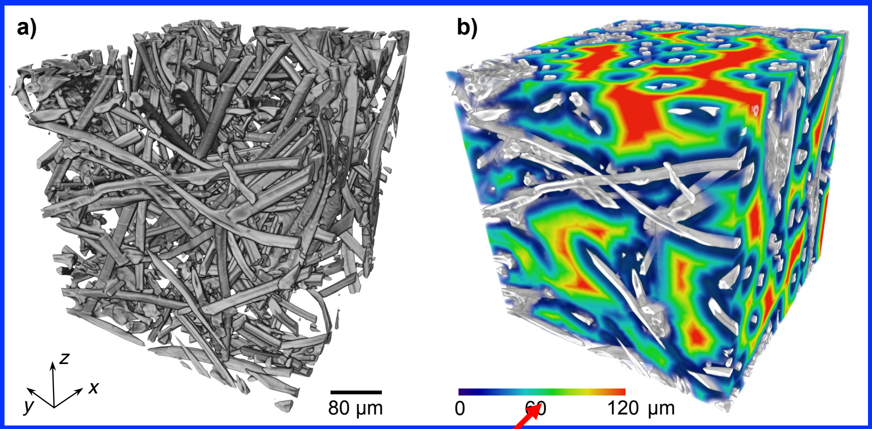

- DSMC: probabilistic simulation method to solve the Boltzmann equation for finite Kn
- Particles motion and collisions are decoupled
- Uses cells and boundaries (Cartesian grid)
- DSMC code: SPARTA (Sandia)

$$\mathrm{Kn} = \lambda / d_p$$

1-5 microns (high T, low P)

$\mathrm{Kn} =$ Knudsen number

$\lambda =$ mean free path

$d_p =$ mean pore diameter

Borner et al. International Journal of Heat and Mass Transfer 106 (2017) 1318–1326

Porous media permeability

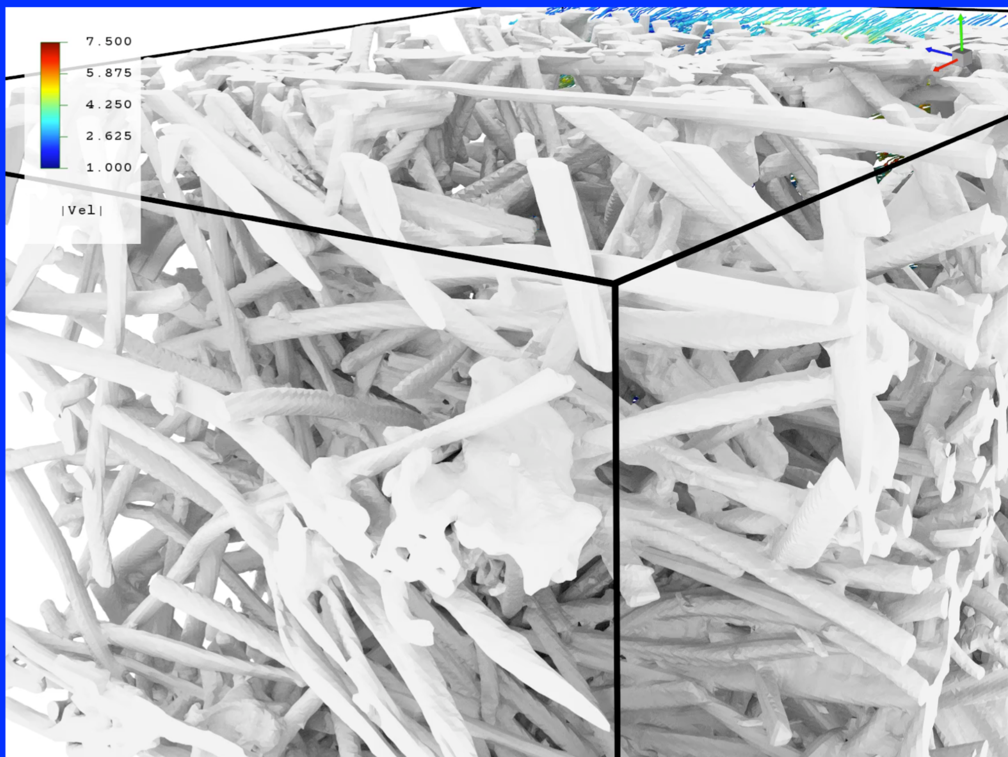

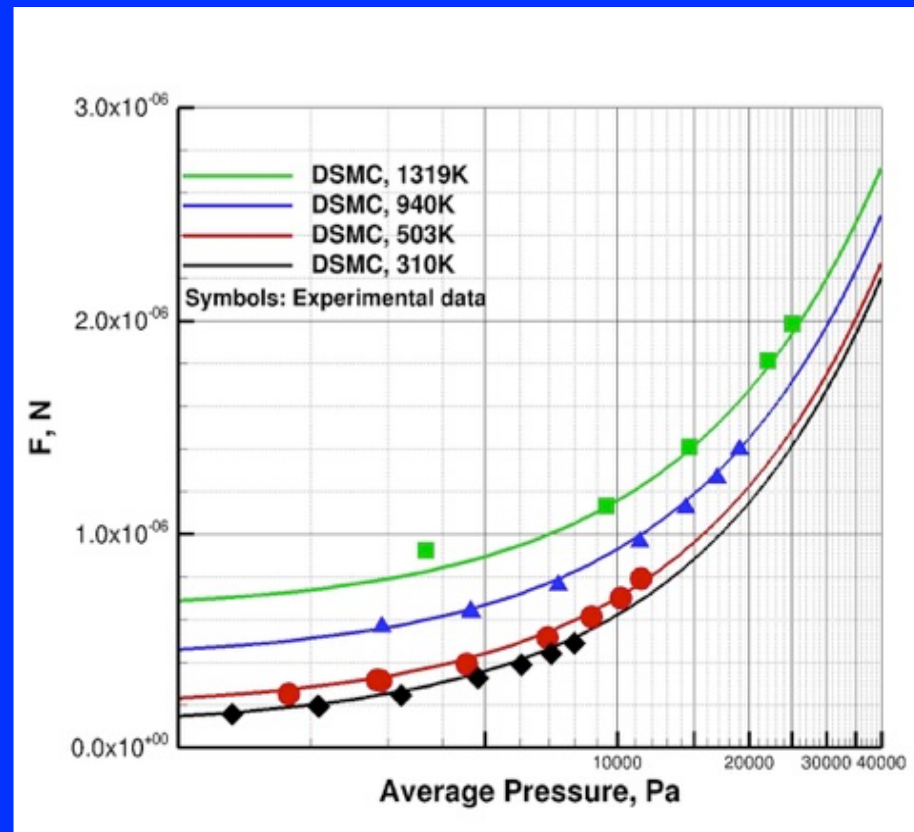

Panerai et al., *Int J Heat Mass Transfer* 101 (2016) 267–273

Borner et al. International Journal of Heat and Mass Transfer 106 (2017) 1318–1326

Building a model for PICA class

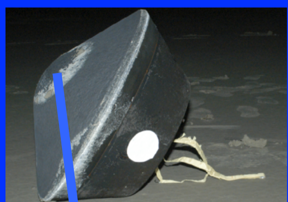

Core - Stardust TPS

Before you do anything in ablation modeling you need:

0. Properties of the material: pyrolysis, conductivity, permeability, etc.
    a. Experimental data
        i. Pyrolysis experiments
        ii. Gas surface interactions data
        iii. Permeability
    b. Micro-computed tomography (microCT) of the material for bulk properties
        i. conductivity
        ii. permeability
        iii. tortuosity
1. Modeling at the macroscale
2. Material response codes
    1. PuMA
    2. PATO
3. Modeling spallation
4. Flow environment coupling

Stardust core image from M. Stackpoole *et al.*, Post-Flight Evaluation of Stardust Sample Return Capsule Forebody Heatshield Material, AIAA 2008-1202

PuMA Development (Ferguson 2017)

Porous Microstructure Analysis (PuMA)

Domain Generation
- Artificial Material Generator
- Micro-tomography Import, Processing, and Thresholding

Visualization
- Marching Cubes
- OpenGL Surface Rendering

Material Properties
- Porosity
- Specific Surface Area
- Effective Thermal Conductivity
- Effective Electrical Conductivity
- Diffusivity / Tortuosity (Bulk and Knudsen)
- Representative Elementary Volume

Material Response
- Oxidation Simulations
- Deposition Model
- Molecuar Beam Simulations
- Transient Heat Transfer

Technical Specifications

- Written in C++
- GUI built on QT
- Parallelized using OpenMP for shared memory systems
- Available at Software.nasa.gov

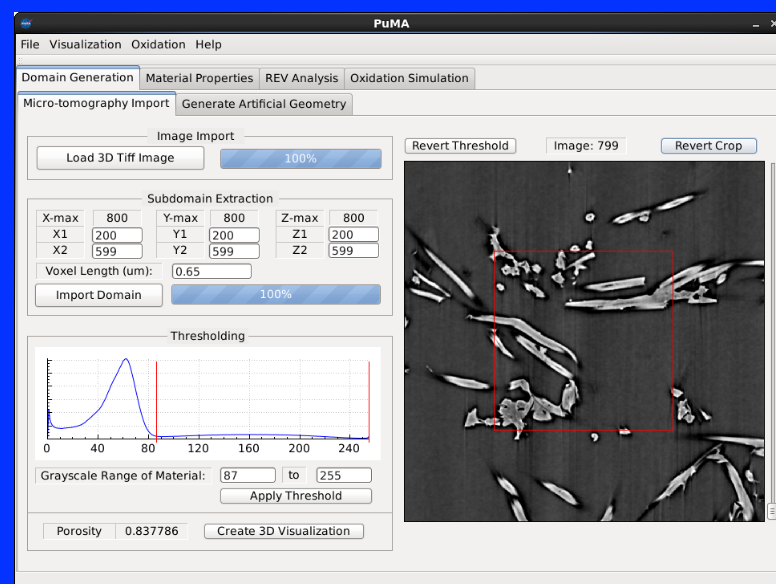

Ferguson, et al. PuMA: the Porous Microstructure Analysis software SoftwareX, Vol 7, January-June, pp. 81-87

PuMA Development

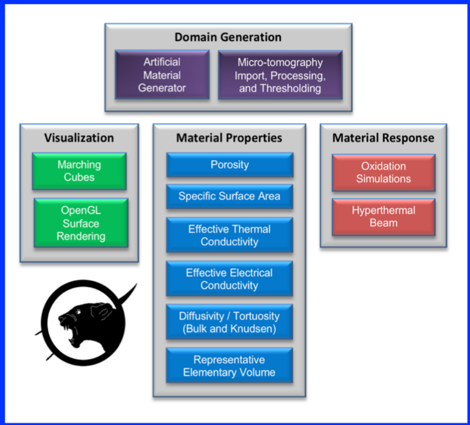

Porous Microstructure Analysis (PuMA) software

Focus of Effort:

Better understanding of material behavior at the microscale

Inform full-scale models to improve NASA's predictive capabilities

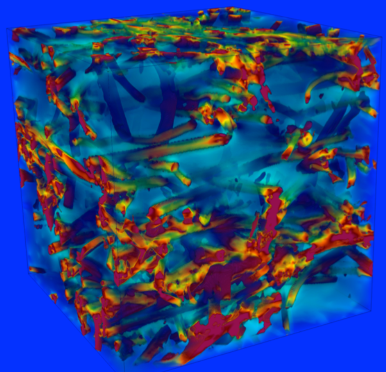
Steady state current flow through porous material

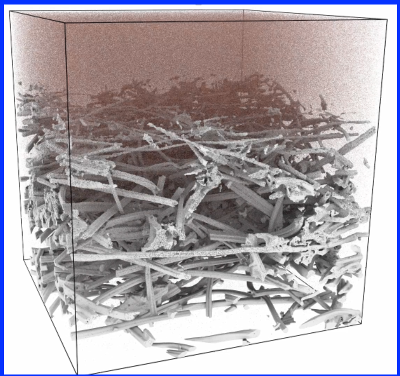
Microscale oxidation simulation in PuMA

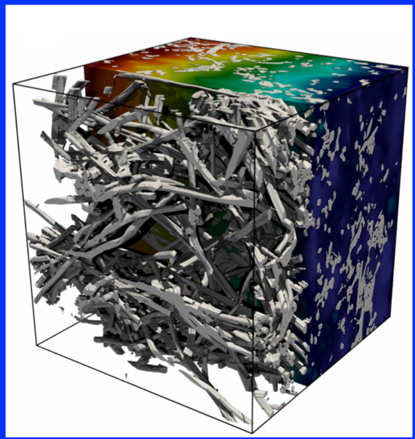
Steady state temperature profile in a porous material

Opens door to computational design of next-generation heat shield materials

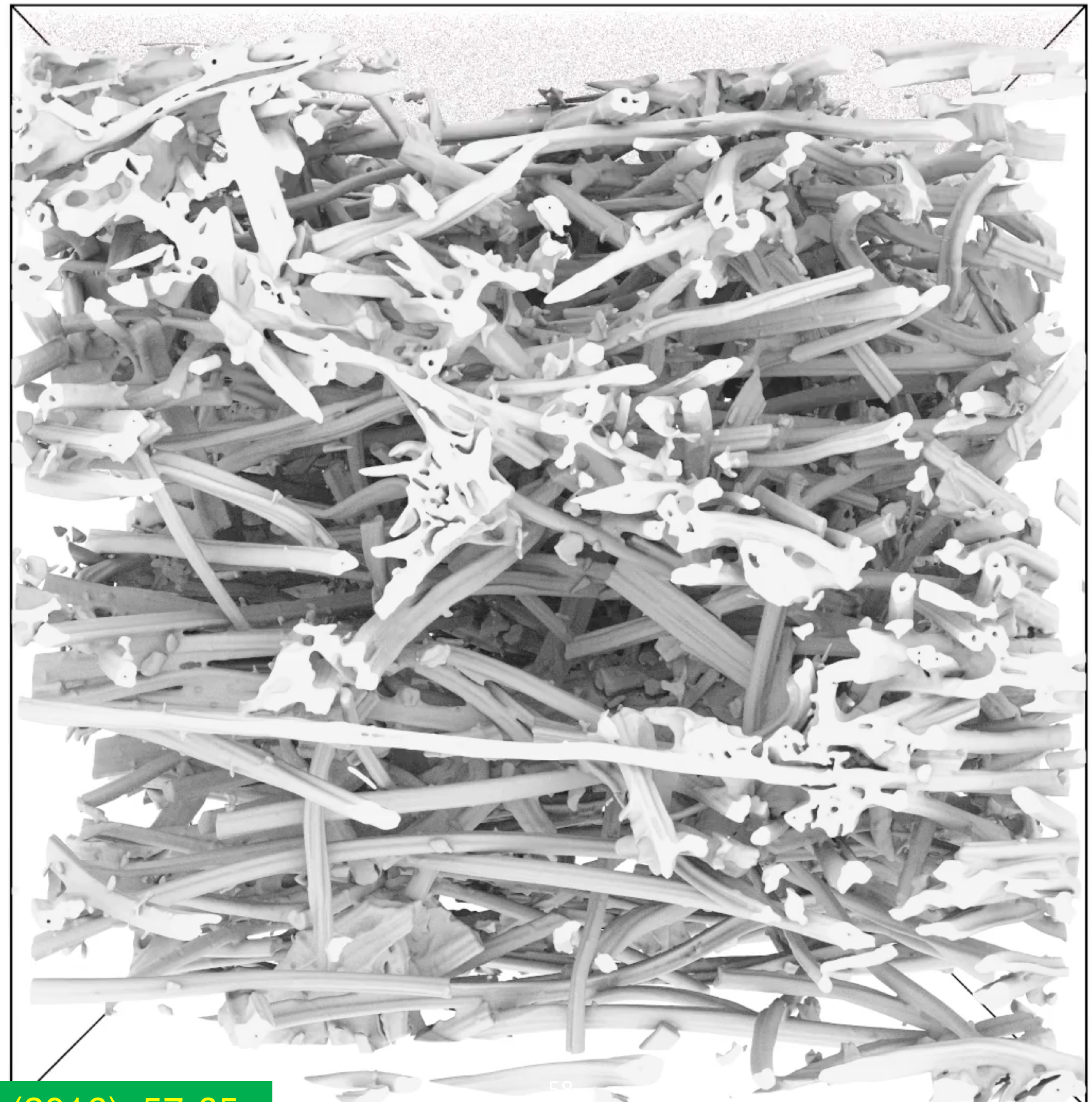

Ferguson et al., *Carbon* 96 (2016), 57-65

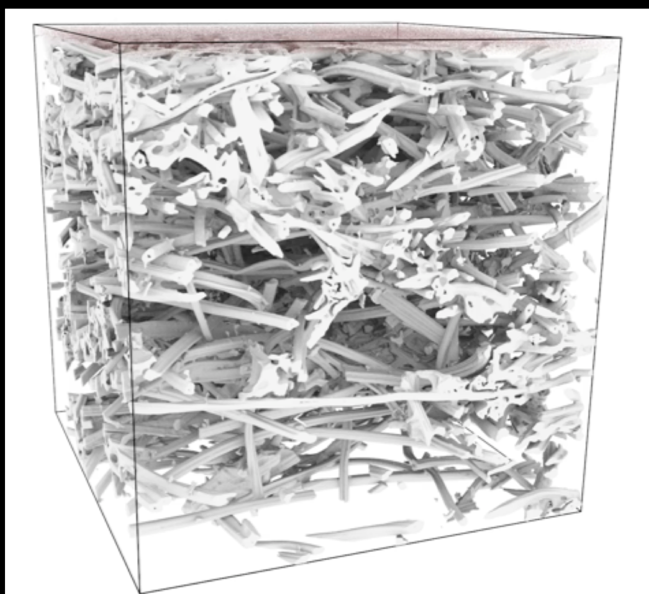

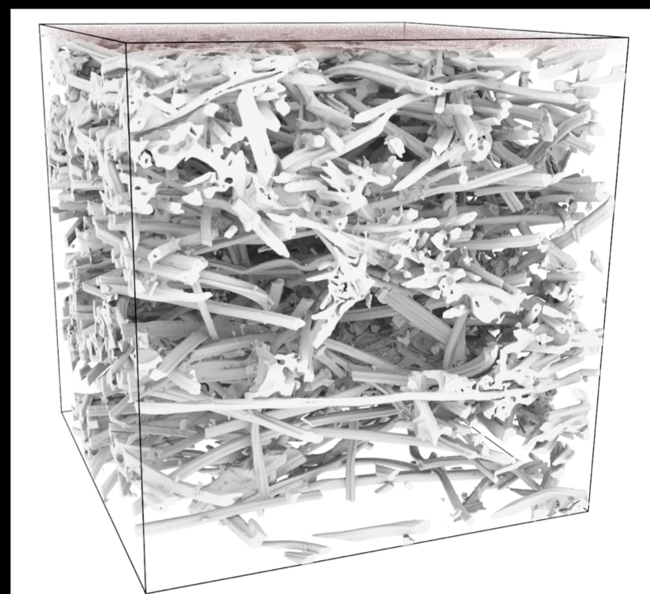

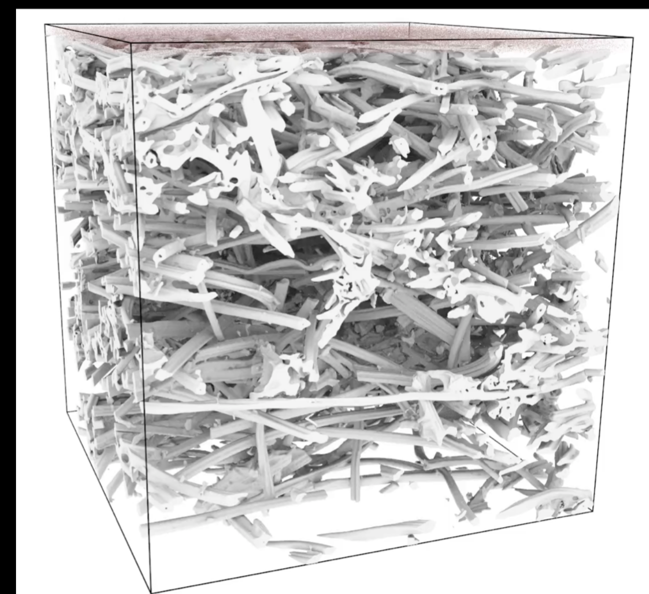

Ferguson et al.,
Carbon 96 (2016),

Advanced Material Generation (Ferguson 2018)

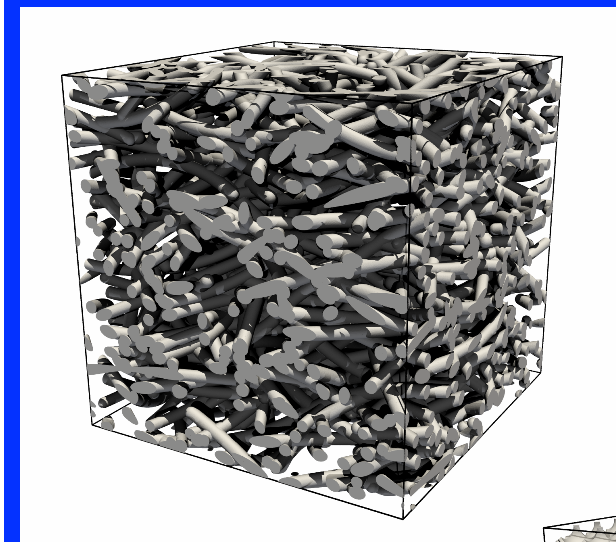

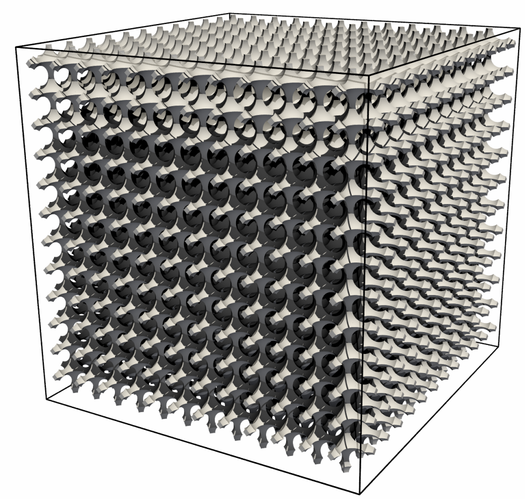

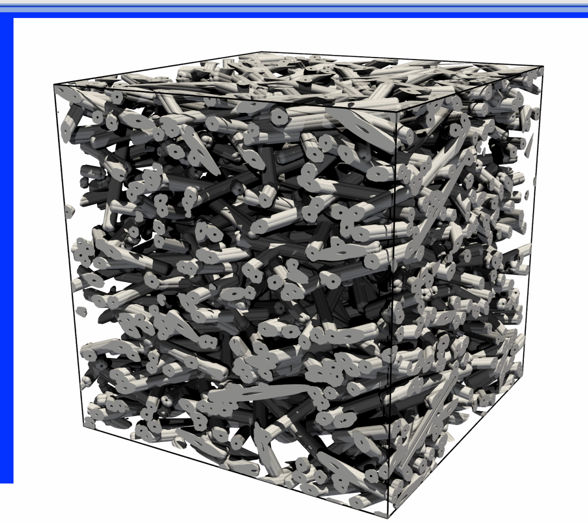

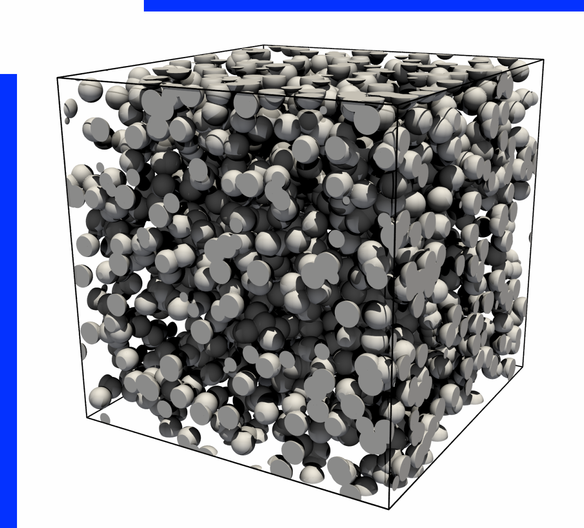

Advanced Material Generation (Ferguson 2018)

Building multilayered weaves

	layers	height	width	ylocation	Tow 1	Tow 2	Tow 3	Tow 4	Tow 5	Tow 6	Tow 7	Tow 8	Tow 9	Tow 10	Tow 11
xlocation					0	0	0	0	5	5	5	10	10	10	10
height					1	1	1	1	1	1	1	1	1	1	1
width					4	4	4	4	4	4	4	4	4	4	4
column 1	3	1	4	0	0	0	1	2	0	1	2	0	1	2	3
column 2	3	1	4	5	0	1	2	3	0	1	2	0	0	1	2
column 3	3	1	4	10	1	2	3	3	1	2	3	0	1	2	3
column 4	3	1	4	15	0	1	2	3	1	2	3	1	2	3	3

- Custom weave diagram format for complex weave design
- TexGen library fully encapsulated
- Design and build 2D and 3D woven structures

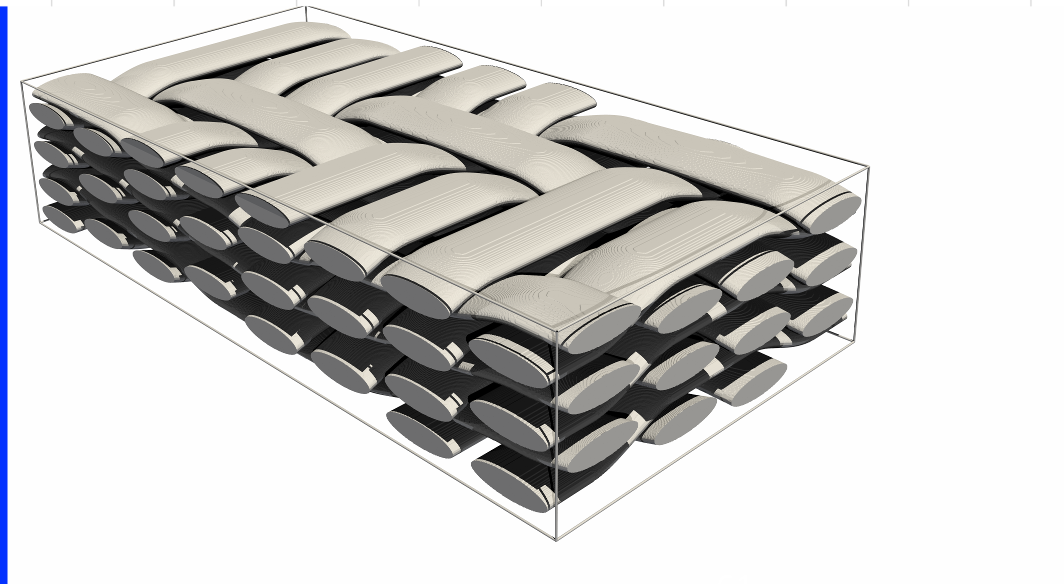

Computing the effective conductivity from microscale to macroscale (Semeraro 2019)

Homogeneous Isotropic:

$$k\left(\frac{\partial^2 T}{\partial x^2}+\frac{\partial^2 T}{\partial y^2}+\frac{\partial^2 T}{\partial z^2}\right)=k\nabla^2 T=0$$

$$T_{left}=T_{right}\rightarrow \text{ at cell surface}$$

$$\left.\frac{\partial T}{\partial n}\right|_{left}=\left.\frac{\partial T}{\partial n}\right|_{right}\rightarrow \text{ at cell surface}$$

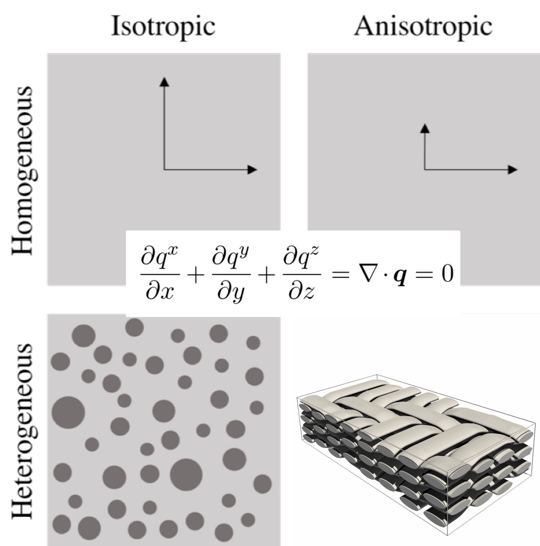

$$\frac{\partial q^x}{\partial x}+\frac{\partial q^y}{\partial y}+\frac{\partial q^z}{\partial z}=\nabla\cdot\boldsymbol{q}=0$$

Requirements
Continuity of temp and flux

Homogeneous Anisotropic:

$$k=\begin{bmatrix}k_{xx} & k_{xy} & k_{xz}\\ k_{yx} & k_{yy} & k_{yz}\\ k_{zx} & k_{zy} & k_{zz}\end{bmatrix}$$

$$k^{ij}=k^{ji}\qquad k^{ii}>0\qquad k^{ii}k^{jj}>{k^{ij}}^2$$

$$k_{xx}\frac{\partial^2 T}{\partial x^2}+k_{xy}\frac{\partial^2 T}{\partial y^2}+k_{xz}\frac{\partial^2 T}{\partial z^2}+$$
$$k_{xy}\frac{\partial^2 T}{\partial x^2}+k_{yy}\frac{\partial^2 T}{\partial y^2}+k_{yz}\frac{\partial^2 T}{\partial z^2}+$$
$$k_{xz}\frac{\partial^2 T}{\partial x^2}+k_{yz}\frac{\partial^2 T}{\partial y^2}+k_{zz}\frac{\partial^2 T}{\partial z^2}=0$$

Heterogeneous Isotropic:

$$\frac{\partial}{\partial x}\left(k(x,y,z)\frac{\partial T}{\partial x}\right)+\frac{\partial}{\partial y}\left(k(x,y,z)\frac{\partial T}{\partial y}\right)+\frac{\partial}{\partial z}\left(k(x,y,z)\frac{\partial T}{\partial z}\right)=0$$

Heterogeneous Anisotropic:

$$\frac{\partial}{\partial x}\left(k_{xx}(x,y,z)\frac{\partial T}{\partial x}+k_{xy}(x,y,z)\frac{\partial T}{\partial y}+k_{xz}(x,y,z)\frac{\partial T}{\partial z}\right)+$$
$$\frac{\partial}{\partial y}\left(k_{xy}(x,y,z)\frac{\partial T}{\partial x}+k_{yy}(x,y,z)\frac{\partial T}{\partial y}+k_{yz}(x,y,z)\frac{\partial T}{\partial z}\right)+$$
$$\frac{\partial}{\partial z}\left(k_{xz}(x,y,z)\frac{\partial T}{\partial x}+k_{yz}(x,y,z)\frac{\partial T}{\partial y}+k_{zz}(x,y,z)\frac{\partial T}{\partial z}\right)=0$$

Effective conductivity of multilayered weave

Building a model for PICA class

Core - Stardust TPS

Stardust core image from M. Stackpoole *et al.,* Post-Flight Evaluation of Stardust Sample Return Capsule Forebody Heatshield Material, AIAA 2008-1202

Before you do anything in ablation modeling you need:

0. Properties of the material: pyrolysis, conductivity, permeability, etc.
   - a. Experimental data
     - i. Pyrolysis experiments
     - ii. Gas surface interactions data
     - iii. Permeability
   - b. Micro-computed tomography (microCT) of the material for bulk properties
     - i. conductivity
     - ii. permeability
     - iii. tortuosity
1. Modeling at the macroscale
2. Material response codes
   1. PuMA
   2. PATO
3. Modeling spallation
4. Flow environment coupling

TGA - revisited

The intrinsic density of phase i in (Type 3) model is given as:

$$\epsilon_i \rho_i = \epsilon_i(0)\rho_i(0) - \sum_{j\in[1,N_R]} \epsilon_i(0)\rho_i(0)F_F\chi_{ij} - \int_0^t \omega_i^h d\tau$$

Summing over all reactions, we get:

$$\epsilon_m \rho_m = \epsilon_m(0)\epsilon\rho_m(0) - \sum_{i\in[1,N_p]} \sum_{j\in[1,N_{R_{P_i}}]} \epsilon_i(0)\rho_i(0)F_{ij}\chi_{ij} - \int_0^t \Omega_h d\tau \quad \text{where:} \quad \Omega_h = \sum_{i\in[1,N_P]} \omega_i^h$$

The SoA (Type 1) model defines the density of the matrix as:

$$\rho_m = \rho_m(0) - \sum_{j\in[1,N_{R_1}]} \rho_i(0)F_{1j}\chi_{1j}$$

Implicit assumptions:

- Volume fraction of matrix does not change vs. Type 3 model where the matrix can shrink or swell
- No heterogeneous reactions

Mass conservation (gas/solid system) (Lachaud 2014-2017)

Type 1, Type 2, Type 3 classification

Type 2 hypothesis: instantaneous transfer of an incompressible gas

$$\partial_x(\dot{m}_g) = -\partial_t(\rho_m)$$

Pyrolysis gas flux

Pyrolysis laws (Arrhenius) = f(Temperature)
- Thermogravimetry analysis (TGA)

Type 2

$$\partial_t(\epsilon_g \rho_g) + \partial_i(\epsilon_g \rho_g v_i^g) = -\partial_t(\rho_m)$$

Open porosity
- Pycnometry
- Tomography

$$\rho_g = \frac{pM}{RT}$$

Momentum Conservation

Pyrolysis laws (Arrhenius)
- Thermogravimetry (TGA)

Type 3

$$\partial_t(\epsilon_g \rho_g) + \partial_i(\epsilon_g \rho_g v_i^g) = -\partial_t(\epsilon_m \rho_m)$$

$$\epsilon_g = 1 - \epsilon_m$$

$$M = \sum_i x_i M_i$$

Momentum Conservation

- pyrometry
- Tomography
- PuMA simulations
- Modeling

- In-situ micro-CT
- PuMA modeling
- Chemistry models

Equilibrium: elemental conservation
Finite rate: species conservation

Realistic Type 3 model developments (Lachaud 2017)

Gas mass & momentum conservations

$$\partial_t(\epsilon_g\rho_g) + \partial_x(\epsilon_g\rho_g v_i^g) = \Pi + \Omega_h$$

evolution of density convection total pyrolysis heterogeneous chemistry

Volume-averaged momentum conservation (Darcy)

$$v_i^g = -\frac{1}{\epsilon_g\mu} K_{ij}\partial_j p$$

gas velocity pressure gradient

Finite-rate chemistry : i species conservations

$$\partial_t(\epsilon_g\rho_g y_i) + \partial_j(\epsilon_g\rho_g y_i v_j^g) + \partial_j\mathcal{F}_{ij} = \pi_{y_i} + \epsilon_g\omega_{y_i}^h$$

evolution of species mass-fraction convection diffusion pyrolysis produced finite-rate chemistry

Equilibrium chemistry : i element conservations

$$\partial_t(\epsilon_g\rho_g z_i) + \partial_j(\epsilon_g\rho_g z_i v_j^g) + \partial_j\mathcal{F}_{ij}^e = \pi_{z_i}$$

evolution of element mass-fraction convection transport pyrolysis produced

Lachaud et al. A generic local thermal equilibrium model for porous reactive materials submitted to high temperatures IJHMT 108 (2017) 1406–1417

Realistic Type 3 model developments (Lachaud 2017)

Energy conservation

$$\partial_t(\rho_t e_t) + \partial_j(\epsilon_g \rho_g h_g v_j^g) + \partial_j \mathcal{Q}_j = \partial_i(k_{ij}\partial_k T) + \mu\epsilon_g^2 k_{ij}^{-1} v_j^g v_i^g$$

where the specific energy of the the solid gas mixture is:

$$\rho_t e_t = \epsilon_g \rho_g e_g + \sum_{\alpha \in [1, N_p]} \epsilon_\alpha \rho_\alpha h_\alpha$$

and

$$\mathcal{Q}_i$$

is the effective diffusive heat flux

Lachaud et al. A generic local thermal equilibrium model for porous reactive materials submitted to high temperatures IJHMT 108 (2017) 1406–1417

Building a model for PICA class

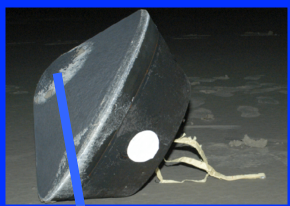

Core - Stardust TPS

Stardust core image from M. Stackpoole *et al.*, Post-Flight Evaluation of Stardust Sample Return Capsule Forebody Heatshield Material, AIAA 2008-1202

Before you do anything in ablation modeling you need:

0. Properties of the material: pyrolysis, conductivity, permeability, etc.
   a. Experimental data
      i. Pyrolysis experiments
      ii. Gas surface interactions data
      iii. Permeability
   b. Micro-computed tomography (microCT) of the material for bulk properties
      i. conductivity
      ii. permeability
      iii. tortuosity
1. Modeling at the macroscale
2. Material response codes
   1. PuMA
   2. PATO
3. Modeling spallation
4. Flow environment coupling

Towards DAO-TPM at the macroscale

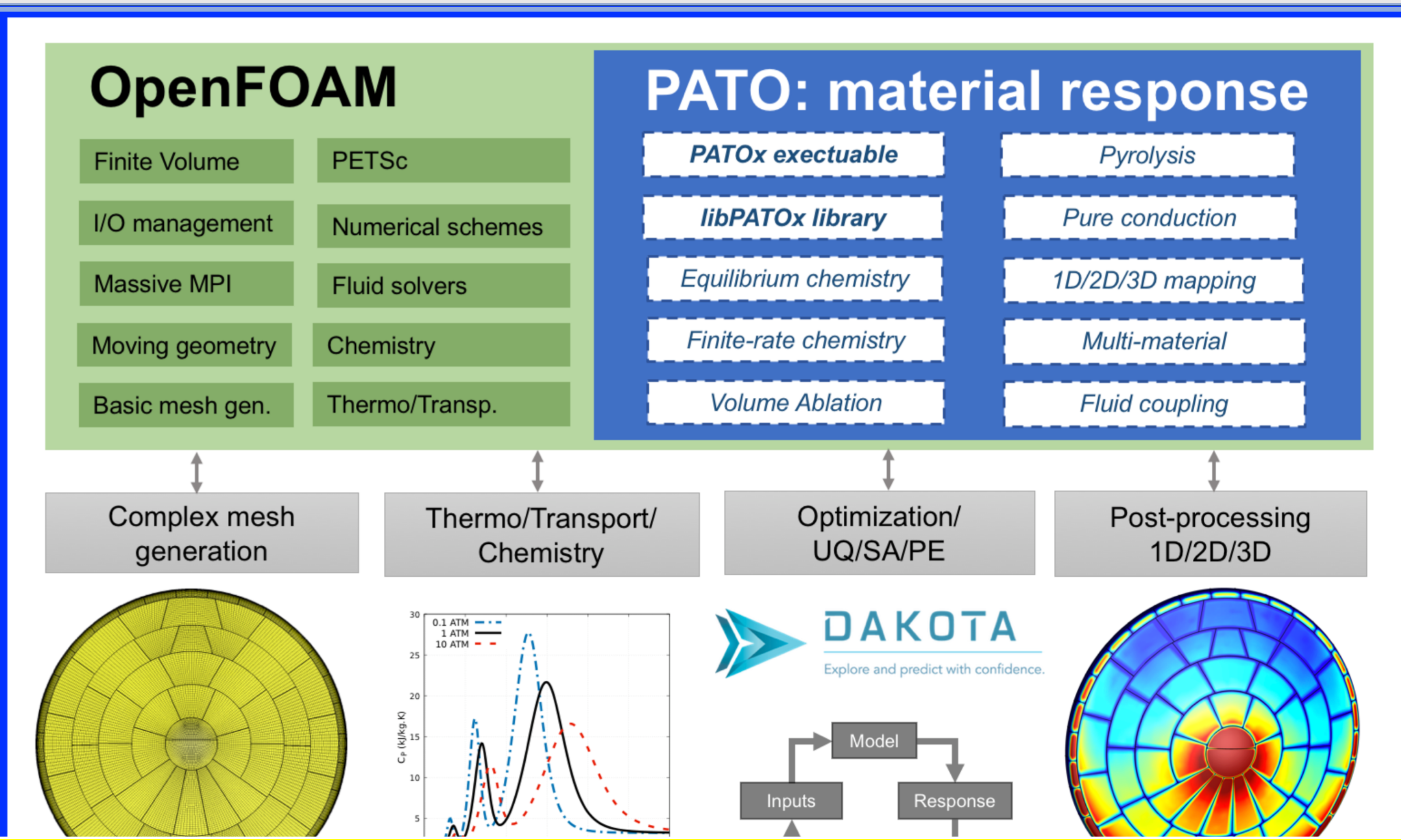

PATO/DAKOTA coupling enables robust uncertainty quantification, sensitivity analysis, model calibration and inverse analysis

Pyroylsis model development methodology

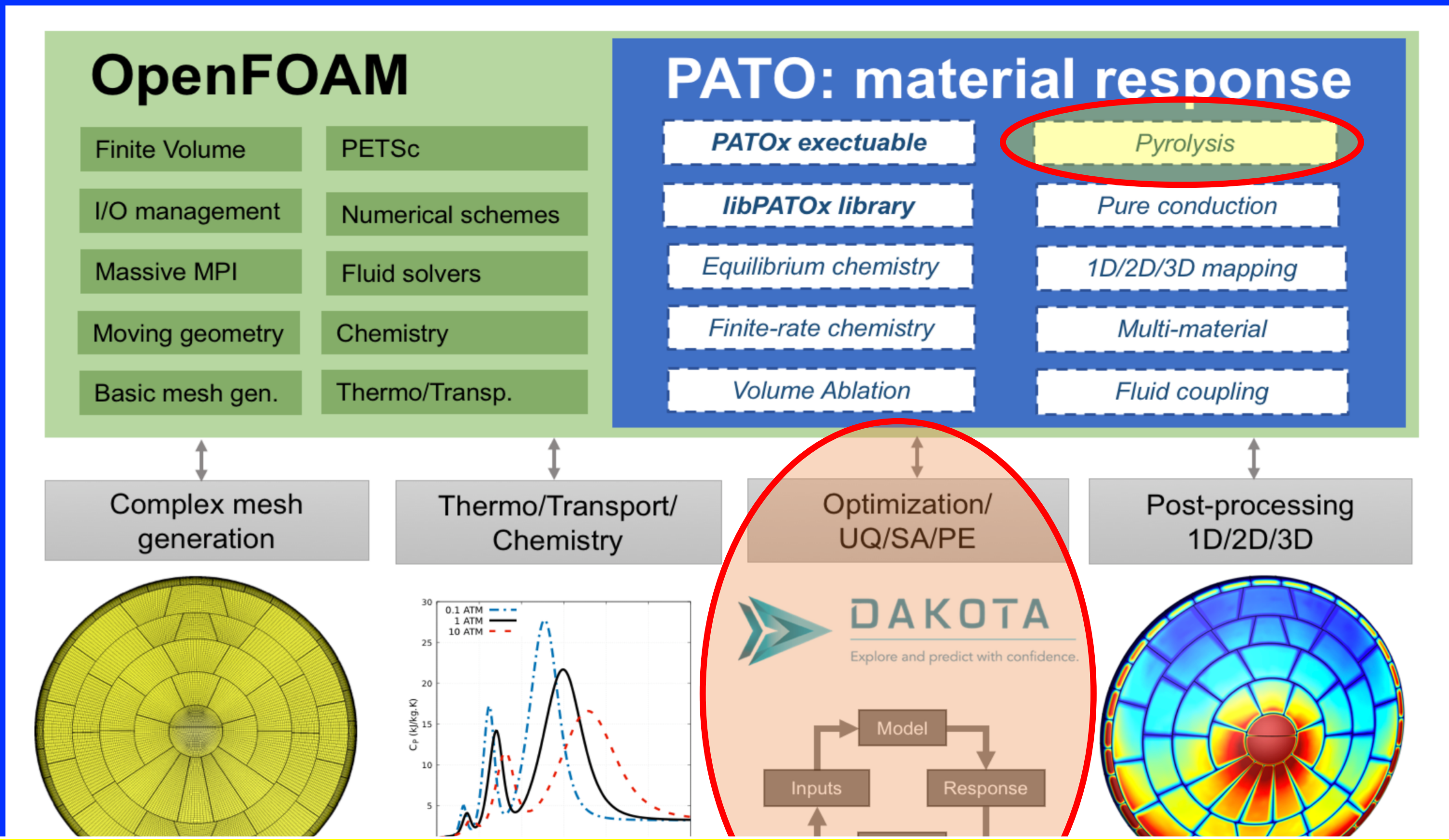

Implementation of material response models is compatible with OpenFOAM software architecture enabling minimum overhead -> fast capabilities

Results – Species production model (Torres 2019)

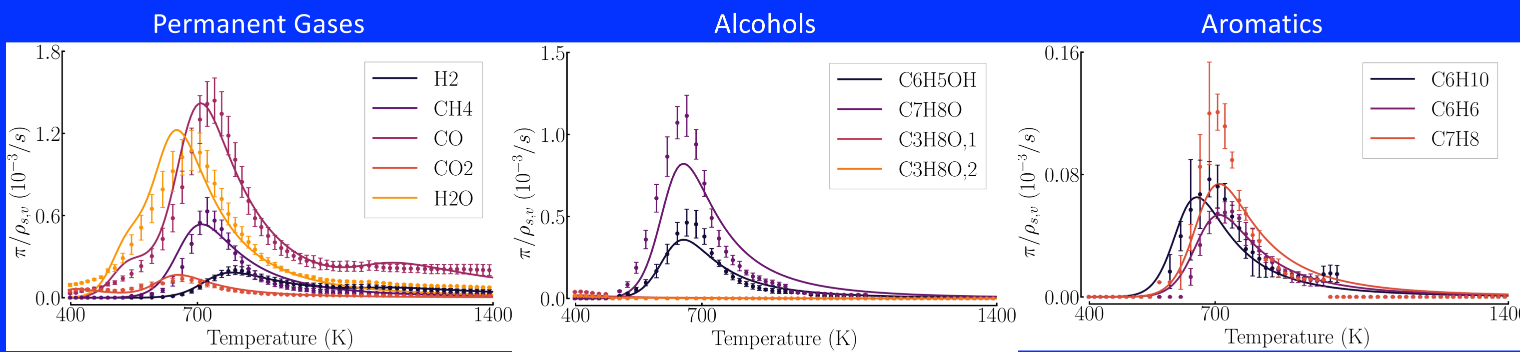

The ρ/ρ_v evolution (TGA curve) can be reconstructed from the optimization

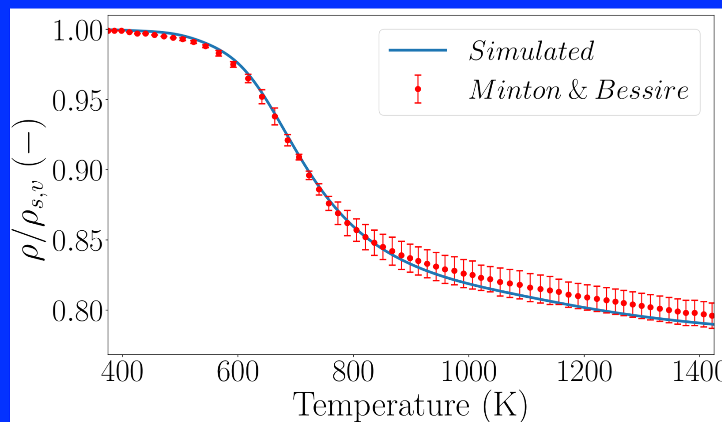

Torres Herrador, *et al.* "A high heating rate pyrolysis model for the Phenolic Impregnated Carbon Ablator (PICA) based on mass spectroscopy experiments," submitted for pub. 2019

Model the MSL entry (Meurisse 2018)

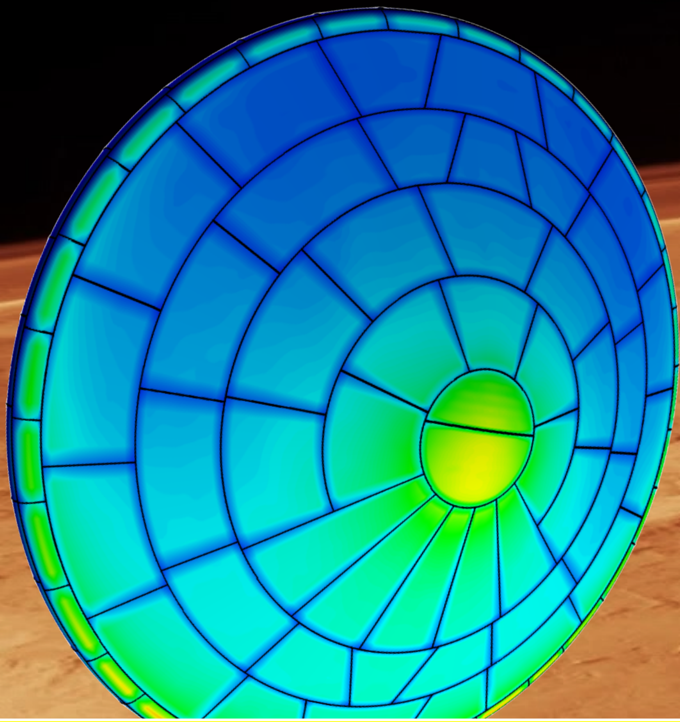

Example use of PATO in V&V mode

Full-scale Mars Science Lab. Tiled Heatshield Material Response

The sizing of the MSL heatshield was verified with FIAT - The question was posed: how well did it do compared to current full 3D with fencing and at the periphery

Meurisse et al. Multidimensional material response simulations of a full-scale tiled ablative heatshield, Aerospace Science and Technology 76 (2018) 497–511

Overview – geometry

MSL PICA heatshield

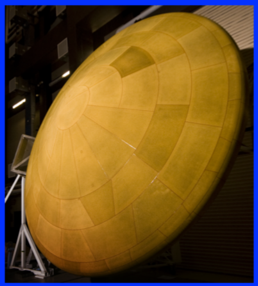

from literature

aeroshell geometry

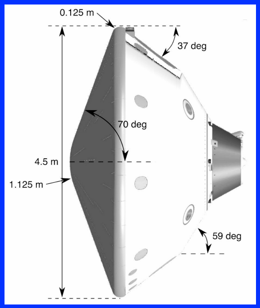

LEGEND

literature

Overview – aerothermal environment

MSL PICA heatshield

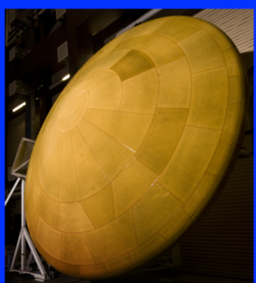

from literature

aeroshell geometry

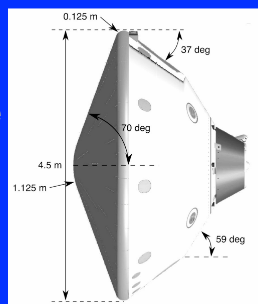

environment meshing
POINTWISE

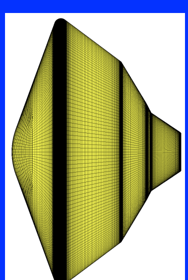

environment mesh

hypersonic CFD
DPLR

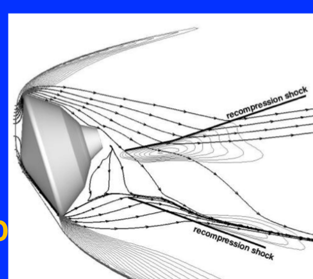

aerothermal environment around aeroshell

boundary layer edges
BLAYER

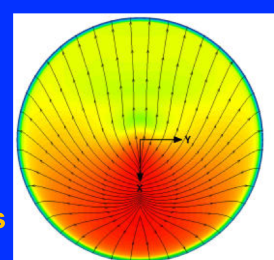

aerothermal environment at the surface

LEGEND

literature
environment

Overview – material response

MSL PICA heatshield

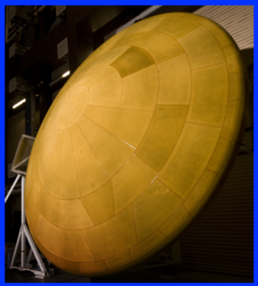

from literature

aeroshell geometry

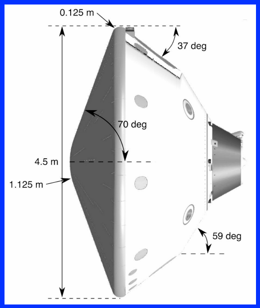

image processing and material meshing POINTWISE

material mesh

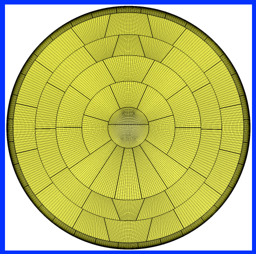

environment meshing POINTWISE

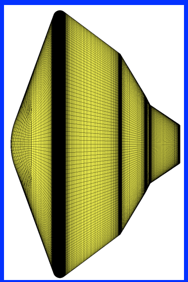

environment mesh

hypersonic CFD DPLR

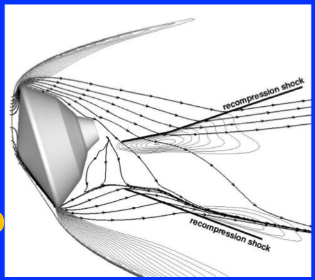

aerothermal environment around aeroshell

boundary layer edges BLAYER

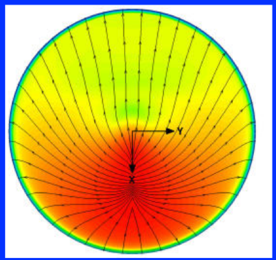

aerothermal environment at the surface

LEGEND

literature
environment
material

Overview – coupling aerothermal environment and material response

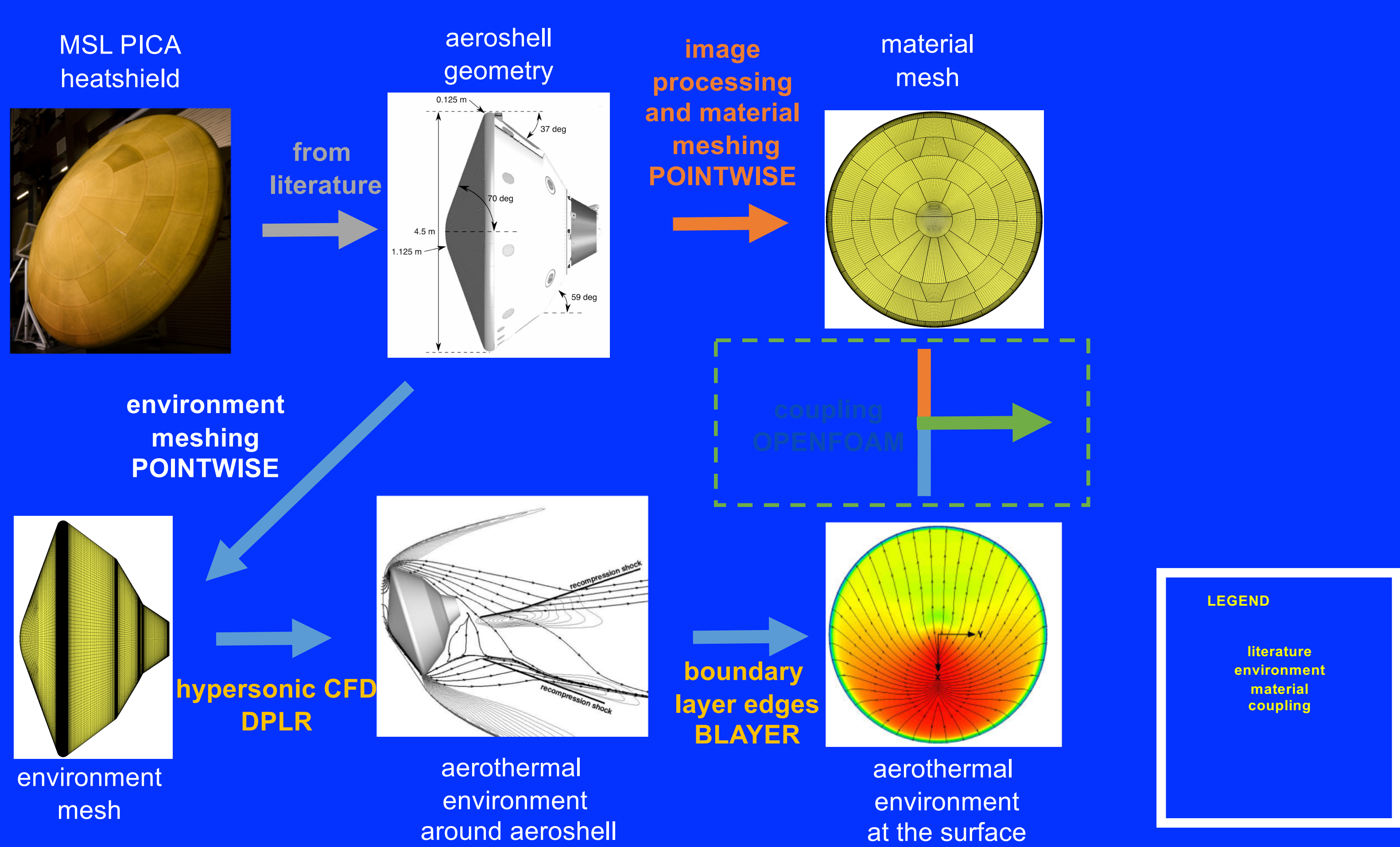

Overview – coupling aerothermal environment and material response

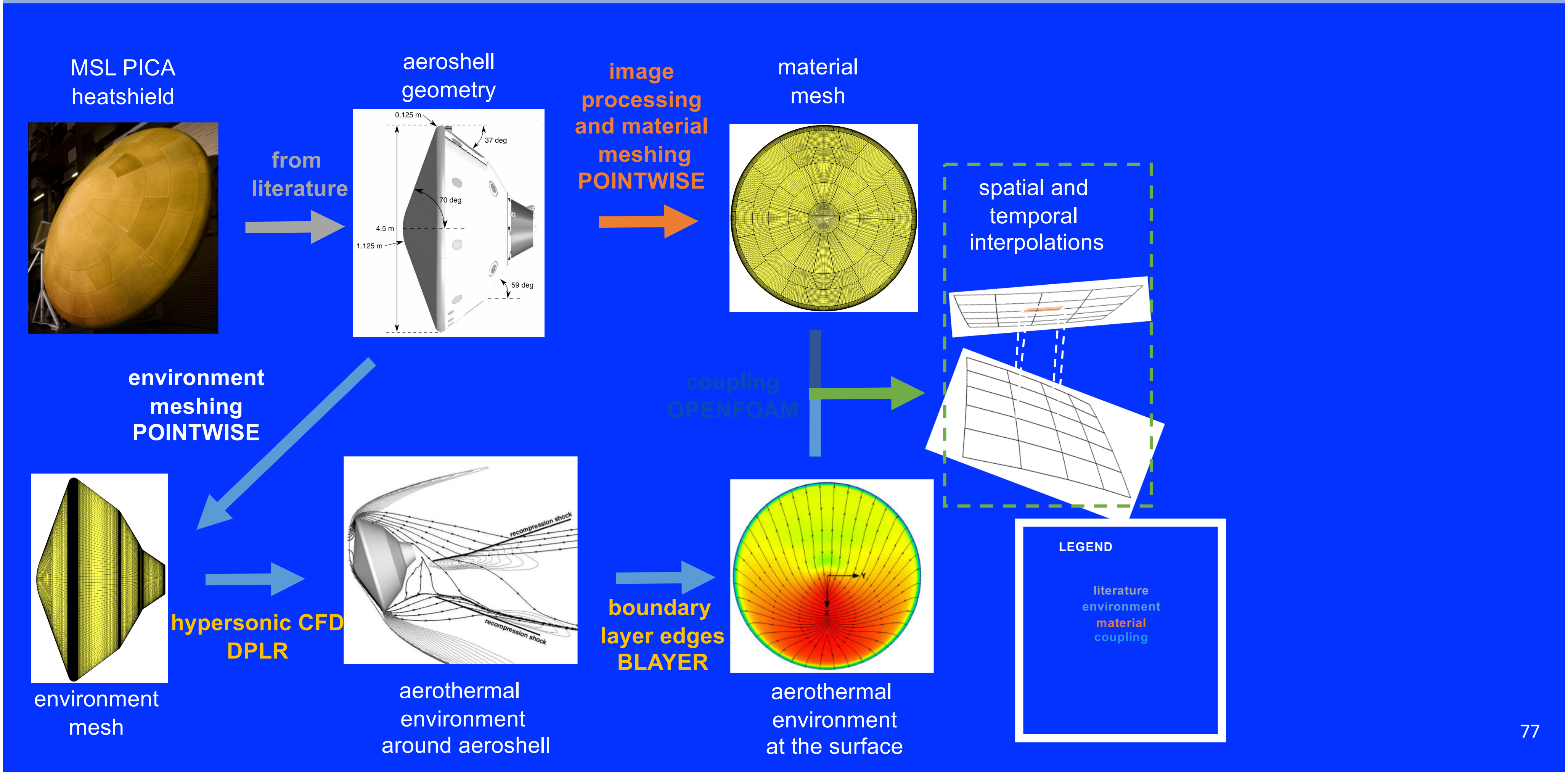

Overview – coupling aerothermal environment and material response

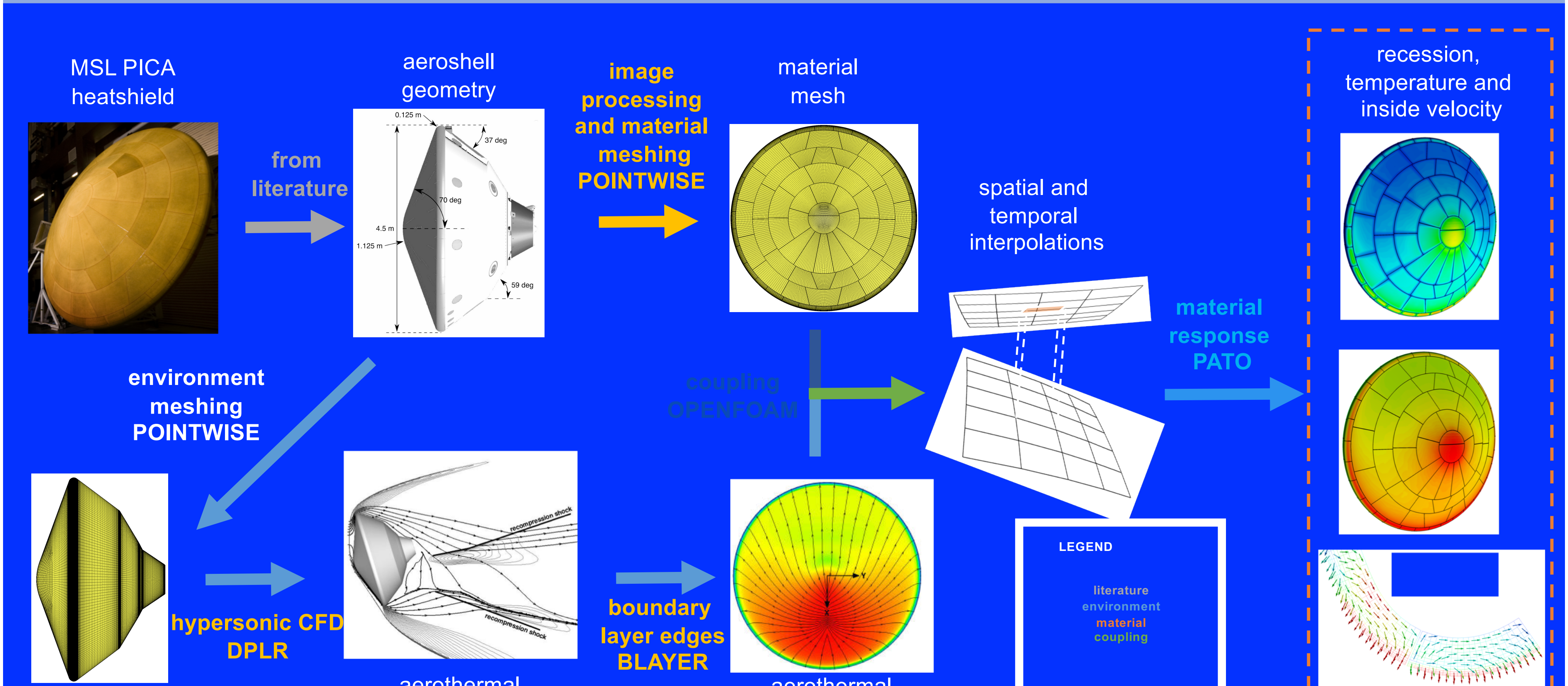

Answer: 1D model did very well except at the periphery with strong curvatures.

PATO simulations of MSL (Meurisse 2018)

New Aerospace Science and Technology article:

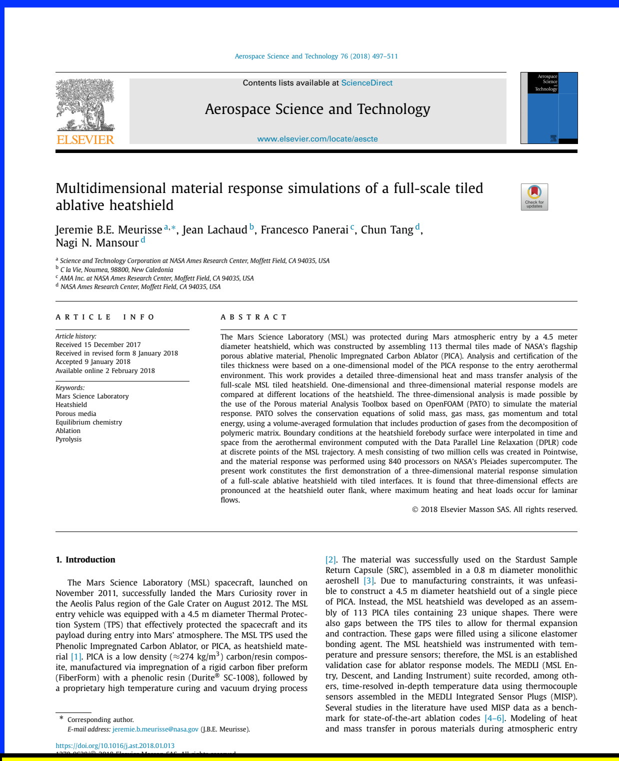
Aerospace Science and Technology 76 (2018) 497–511

Contents lists available at ScienceDirect

Aerospace Science and Technology

www.elsevier.com/locate/aescte

Multidimensional material response simulations of a full-scale tiled ablative heatshield

Jeremie B.E. Meurisse [a,*], Jean Lachaud [b], Francesco Panerai [c], Chun Tang [d], Nagi N. Mansour [d]

[a] Science and Technology Corporation at NASA Ames Research Center, Moffett Field, CA 94035, USA
[b] C la Vie, Noumea, 98800, New Caledonia
[c] AMA Inc. at NASA Ames Research Center, Moffett Field, CA 94035, USA
[d] NASA Ames Research Center, Moffett Field, CA 94035, USA

ARTICLE INFO

Article history:
Received 15 December 2017
Received in revised form 8 January 2018
Accepted 9 January 2018
Available online 2 February 2018

Keywords:
Mars Science Laboratory
Heatshield
Porous media
Equilibrium chemistry
Ablation
Pyrolysis

ABSTRACT

The Mars Science Laboratory (MSL) was protected during Mars atmospheric entry by a 4.5 meter diameter heatshield, which was constructed by assembling 113 thermal tiles made of NASA's flagship porous ablative material, Phenolic Impregnated Carbon Ablator (PICA). Analysis and certification of the tiles thickness were based on a one-dimensional model of the PICA response to the entry aerothermal environment. This work provides a detailed three-dimensional heat and mass transfer analysis of the full-scale MSL tiled heatshield. One-dimensional and three-dimensional material response models are compared at different locations of the heatshield. The three-dimensional analysis is made possible by the use of the Porous material Analysis Toolbox based on OpenFOAM (PATO) to simulate the material response. PATO solves the conservation equations of solid mass, gas mass, gas momentum and total energy, using a volume-averaged formulation that includes production of gases from the decomposition of polymeric matrix. Boundary conditions at the heatshield forebody surface were interpolated in time and space from the aerothermal environment computed with the Data Parallel Line Relaxation (DPLR) code at discrete points of the MSL trajectory. A mesh consisting of two million cells was created in Pointwise, and the material response was performed using 840 processors on NASA's Pleiades supercomputer. The present work constitutes the first demonstration of a three-dimensional material response simulation of a full-scale ablative heatshield with tiled interfaces. It is found that three-dimensional effects are pronounced at the heatshield outer flank, where maximum heating and heat loads occur for laminar flows.

1. Introduction

The Mars Science Laboratory (MSL) spacecraft, launched on November 2011, successfully landed the Mars Curiosity rover in the Aeolis Palus region of the Gale Crater on August 2012. The MSL entry vehicle was equipped with a 4.5 m diameter Thermal Protection System (TPS) that effectively protected the spacecraft and its payload during entry into Mars' atmosphere. The MSL TPS used the Phenolic Impregnated Carbon Ablator, or PICA, as heatshield material [1]. PICA is a low density (≈274 kg/m^3) carbon/resin composite, manufactured via impregnation of a rigid carbon fiber preform (FiberForm) with a phenolic resin (Durite® SC-1008), followed by a proprietary high temperature curing and vacuum drying process [2]. The material was successfully used on the Stardust Sample Return Capsule (SRC), assembled in a 0.8 m diameter monolithic aeroshell [3]. Due to manufacturing constraints, it was unfeasible to construct a 4.5 m diameter heatshield out of a single piece of PICA. Instead, the MSL heatshield was developed as an assembly of 113 PICA tiles containing 23 unique shapes. There were also gaps between the TPS tiles to allow for thermal expansion and contraction. These gaps were filled using a silicone elastomer bonding agent. The MSL heatshield was instrumented with temperature and pressure sensors; therefore, the MSL is an established validation case for ablator response models. The MEDLI (MSL Entry, Descent, and Landing Instrument) suite recorded, among others, time-resolved in-depth temperature data using thermocouple sensors assembled in the MEDLI Integrated Sensor Plugs (MISP). Several studies in the literature have used MISP data as a benchmark for state-of-the-art ablation codes [4–6]. Modeling of heat and mass transfer in porous materials during atmospheric entry

* Corresponding author.
E-mail address: jeremie.b.meurisse@nasa.gov (J.B.E. Meurisse).

https://doi.org/10.1016/j.ast.2018.01.013

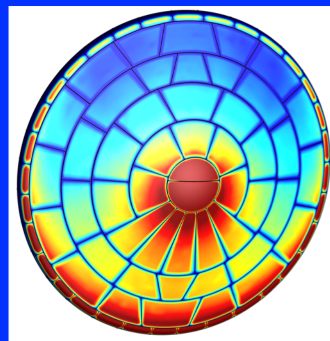

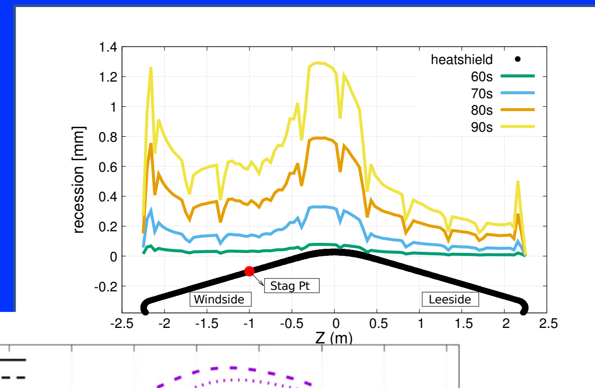

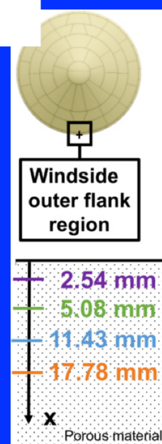

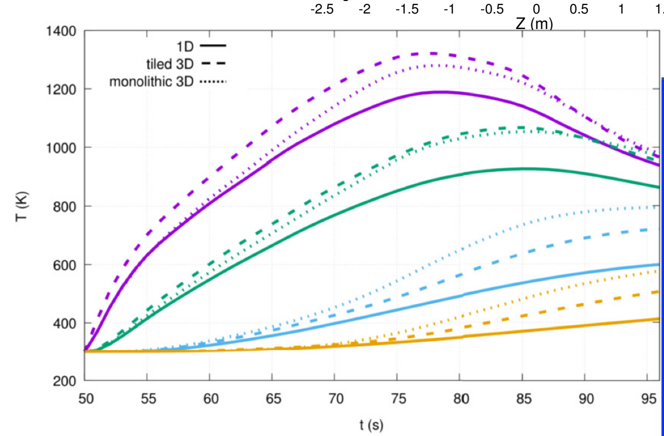

First material response simulation of a full-scale tiled ablative heatshield.
PATO optimized for supercomputing simulation

Meurisse et al. Multidimensional material response simulations of a full-scale tiled ablative heatshield, Aerospace Science and Technology 76 (2018) 497–511

What was not covered

Stardust core image from M. Stackpoole *et al.*, Post-Flight Evaluation of Stardust Sample Return Capsule Forebody Heatshield Material, AIAA 2008-1202

Before you do anything in ablation modeling you need:

0. Properties of the material: pyrolysis, conductivity, permeability, etc.
   a. Experimental data
      i. Pyrolysis experiments
      ii. Gas surface interactions data
      iii. Permeability
   b. Micro-computed tomography (microCT) of the material for bulk properties
      i. conductivity
      ii. permeability
      iii. tortuosity
1. Modeling at the macroscale
2. Material response codes
   1. PuMA
   2. PATO
3. Modeling spallation
4. Flow environment + Materials response coupling

Challenges: spallation, intumescence+ many others

Spallation: Surface recession due to breakup of fibers

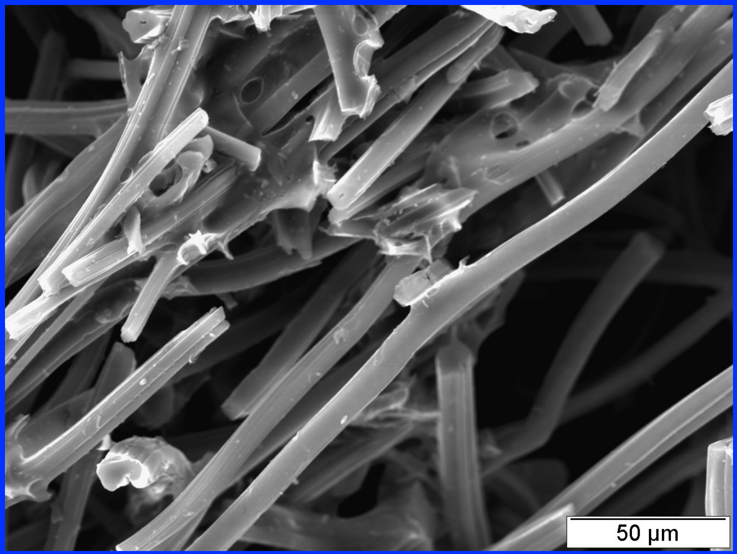

Virgin

- Fibers diameter ~ 9-13 µm
- Fibers length ~ 100-600 µm
- Bundles or cluster of multiple fibers

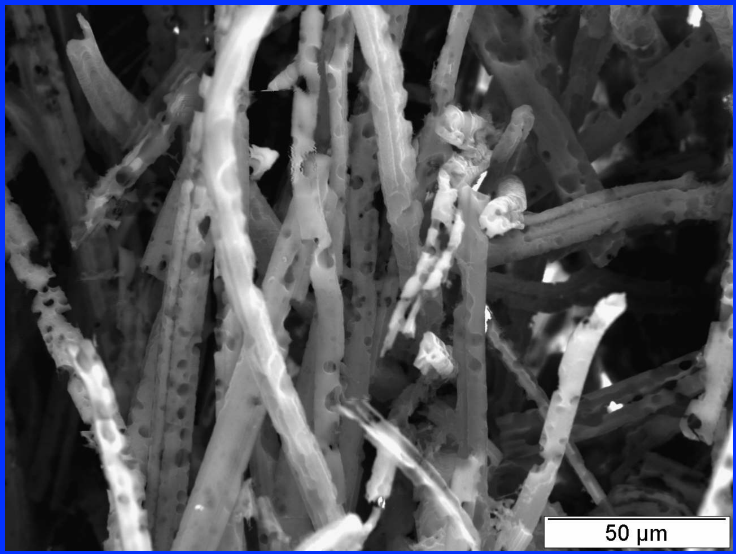

Oxidized

- Oxidation at "active sites" resulting in pitting patterns on the fiber surface
- Uniform thinning along the length